Eur. J. Mineral.
2007, **19**, 513–532
Published online August 2007

The Miocene granitoid rocks of Mt. Bukulja (central Serbia): evidence for pannonian extension-related granitoid magmatism in the northern Dinarides

VLADICA CVETKOVIĆ[1,*], GIAMPIERO POLI[2], GEORGE CHRISTOFIDES[3], ANTONIS KORONEOS[3], ZOLTAN PÉCSKAY[4], KRISTINA RESIMIĆ-ŠARIĆ[1] and VLADISAV ERIĆ[5]

[1] Faculty of Mining and Geology, University of Belgrade, Đušina 7, 11000 Belgrade, Serbia
*Corresponding author, e-mail: cvladica@mkpg.rgf.bg.ac.yu
[2] Department of Earth Sciences, University of Perugia, Piazza Universita', 06100 Perugia, Italy
[3] Faculty of Sciences, School of Geology, Department of Mineralogy, Petrology and Economic Geology, Aristotle University, Thessaloniki, Greece
[4] Institute of Nuclear Research of the Hungarian Academy of Sciences (ATOMKI), Bem ter 18/c, 41001 Debrecen, Hungary
[5] RIO SAVA Exploration, Bulevar Mihajla Pupina 10i, 11000 Belgrade, Serbia

Abstract: The study presents evidence about the origin and evolution of the Miocene (20–17 Ma) granitoid pluton of Mt. Bukulja, situated within the southern Pannonian/northern Dinarides region (central Serbia, south-central Europe). The pluton is composed of slightly peraluminous two-mica granite (TMG), metaluminous hornblende-biotite and biotite-bearing (H-BG) granite and rare aplite granite. A lamprophyre dyke (BLD) similar in composition and age to other Serbian primitive minettes has been found in the vicinity of Mt. Bukulja. The available and newly determined radiometric age suggests that the TMG was emplaced around 20 Ma whereas the age of the H-BG is inadequately constrained. TMG and H-BG show similar petrographic characteristics but evidence of open system magma processes is found only in the H-BG. In comparison to the H-BG, the TMGs are less enriched in most trace elements, including REE, and have a more fractionated REE-pattern and stronger negative Eu-anomaly. The TMGs display a wider range of initial Sr-Nd isotope ratios ($^{87}Sr/^{86}Sr_{20\,Ma}$ = 0.70652–0.71368 and $^{143}Nd/^{144}Nd_{20\,Ma}$ = 0.51223–0.51283) than the H-BG ($^{87}Sr/^{86}Sr_{20\,Ma}$ = 0.70768–0.70781 and $^{143}Nd/^{144}Nd_{20\,Ma}$ = 0.51242–0.51256). Geochemical modeling suggests that the H-BG could have derived from a BLD-like melt by mixing plus fractionation processes assuming a batch of TMG-like magma as the acid end-member. On the other hand, the geochemical variability of the TMG is reproduced by an AFC model with an assimilation/fractionation ratio (r) of 0.5 and with high amount of crustal component (~20–50 %) starting from the least evolved TMG rocks. In the modeling, the average composition of the least evolved TMG samples was used to represent the parental magma composition whereas the composition of adjacent metamorphic rocks was adopted as possible contaminant. The composition of the least evolved TMG implies that the TMG parental magma likely originated by melting of a mafic lithology such as earlier basalts underplating in the lower crust. The high proportions of crustal assimilation along with other geochemical and geological evidence suggest that the Mt. Bukulja TMG originated within the same geotectonic setting as acid volcanics of the north Pannonian Basin. The results of this study support the hypothesis that the Mt. Bukulja pluton is related to tectonomagmatic events controlled by the early extensional phases in the opening of the Pannonian basin.

Key-words: granite, peraluminous, assimilation, crust, Balkan Peninsula, igneous petrology, geochemistry.

Introduction

Granite petrogenesis has been demonstrated to be an important tool not only to understand crust evolution but also to constrain geodynamic conditions and/or specific tectonic changes in the existence of an orogen (*e.g.* Rottura *et al.*, 1997; Pe-Piper, 2000; Schofield & D'Lemos, 2000; Perugini *et al*., 2004; Christofides *et al*., 2007).

In the Pannonian – Carpathian – Dinaride area two series of granitoids crop out: i) Late Oligocene granitoids in the Dinarides, which are generally considered as the southern continuation of the Periadriatic calc-alkaline magmatism (von Blanckenburg & Davies, 1995; Pamić, 1993; Pamić & Balen, 2001), and ii) Miocene granitoids which are supposed to be related to the early extensional phases in the Pannonian-Carpathian basin (Karamata *et al*., 1990;

DOI: 10.1127/0935-1221/2007/0019-1736
0935-1221/07/0019-1736 $ 9.00

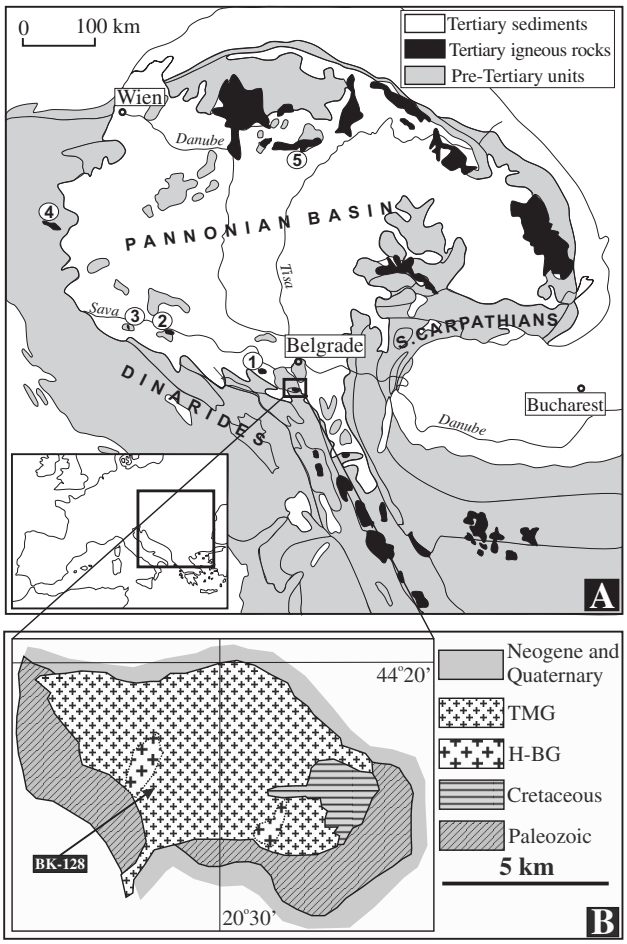

Fig. 1. Geological sketch of the Mt. Bukulja pluton (B) and a simplified geological sketch map of the Pannonian-Carpathian-Dinaride area (A). The position of the Mt. Bukulja granitoid is squared; the locations of other granitoids situated along the Southern margin of the Pannonian Basin (1 – Mt. Cer, 2 – Mt. Motajica, 3 – Mt. Prosara and 4 – Mt. Pohorje) as well as the position of Early/Middle Miocene acid rocks of the northern Pannonian Basin (5) are also shown. TMG, two mica granite; H-BG, hornblende-biotite- and biotite-bearing granites. Hornblende-biotite granite is found only in a drill-core (BK128).

Cvetković *et al*., 2004a). The two suites differ mainly for: i) their position in respect to the Pannonian Basin, the latter being very close to the southern margin of the basin; ii) having mostly metaluminous and peraluminous character, respectively; and iii) displaying Pb/Zn ± Ag ± Sb and U-Nb-Ta-Sn metallogenetic features, respectively (*e.g.* Karamata *et al*., 1990; Erić, 1999).

The Miocene suite consists of Mt. Bukulja and Mt. Cer plutons in Serbia (locality 1 in Fig. 1A), few granitoid bodies situated further north (localities 2, 3 in Fig. 1A), and Mt. Pohorje granite in Slovenia (locality 4 in Fig. 1A). All these plutons are similar on the basis of geochemical characteristics and Miocene age (Knežević *et al*., 1989; Karamata *et al*., 1990; Trajanova *et al*., 2005).

In this study we present and discuss new geochemical data on Mt. Bukulja granitoid rocks, including whole-rock REE and Sr-Nd isotope analyses. In addition, we present new K/Ar ages and discuss all the available age data taking into account the major tectonomagmatic events in the Pannonian Basin. Geochemical and age data aim to decipher genesis and evolution of the Mt. Bukulja granitoids, and to discuss their geodynamic setting with respect to the Pannonian Basin extension.

Geology and petrography of the Mt. Bukulja pluton

The Mt. Bukulja pluton crops out about 60 km south of Belgrade and covers an area of about 40 km^2 (Fig. 1B). It is an E-W trending granitic body which is intensively ruptured by predominantly ESE-WNW oriented fractures. In the west, the pluton intrudes low-grade Devonian/Carboniferous schists of the Jadar Block terrane (Karamata *et al*., 1994), whereas in the east it intrudes a Cretaceous sedimentary series, producing a 3 km wide contact metamorphic zone composed of skarns and garnetites. Taking into account that the Cretaceous sediments underwent no previous regional metamorphism, it can be suggested that the Bukulja pluton intruded very shallow crustal levels (< 5 km). The southern part of the granitic mass is covered by Neogene sediments, which accumulated within a tectonic depression and consist of interlayered sandstones, clays, and coarse-grained clastites containing granitic and metamorphic blocks.

The bulk of the granitoid mass is represented by a medium-grained to slightly porphyritic two-mica granite that locally grades to microgranite facies. Biotite granites are subordinate and generally occur as isolated outcrops, without observable relations with the two-mica granite. Only very rarely, the biotite granites appear as patches of various dimensions (from several decimeters to several tens of meters) within the rocks, showing relatively sharp contacts with the host rocks. The above mentioned granite facies are frequently cut by pegmatitic and aplitic veins, the latter showing transitions to aplitic granites. In addition, a hornblende-bearing granite sample was recovered from a drill-core (Fig. 1B).

Near the western margin of the Mt. Bukulja granite body a lamprophyric dyke was found (hereafter BLD, Bukulja Lamprophyric Dyke). It is a porphyritic melanocratic rock composed of altered phlogopite and sericitized plagioclase in a groundmass of serpentine minerals and calcite. Although the rock exhibits altered mineralogy, it shows a similar K/Ar age (26 Ma on phlogopite; Cvetković *et al*., 2004b), as well as similar geochemical characteristics to other primitive minettes found in the region (Prelević *et al*., 2005).

The Mt. Bukulja rocks are classified in terms of the Q'-ANOR diagram of Streckeisen & Le Maitre (1979) (Fig. 2A), and on the basis of modal composition in Table 1. The rocks containing muscovite are named two-mica granite (hereafter TMG), whereas the muscovite-free samples are named biotite granite and hornblende-biotite granite. Owing to the common geochemical and petrographical features (see below) hornblende-biotite- and

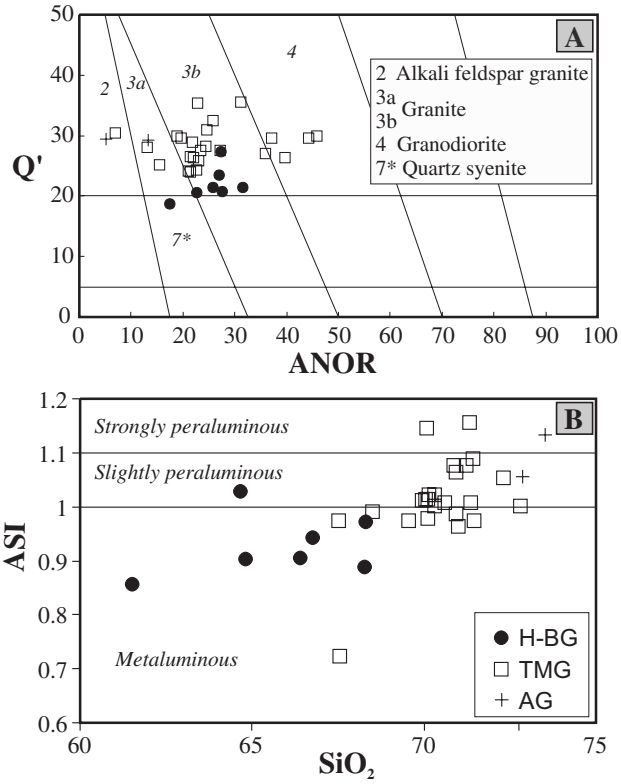

Fig. 2. A: Representative rock compositions of the Bukulja pluton plotted in Q'ANOR classification diagram. B: SiO_2 wt.% *vs.* Alumina Saturation Index (ASI = molecular Al/(Ca+K+Na) plot.

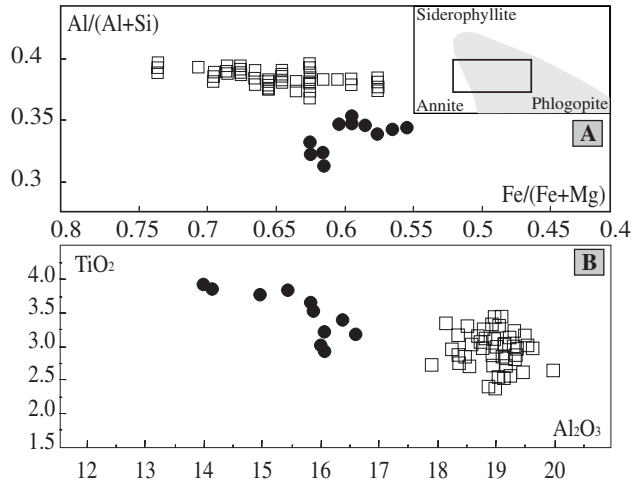

Fig. 3. Chemical compositions for biotite of the Mt. Bukulja granitoid rocks. (A) Enlarged portion of the quadrilateral classification diagram for biotites (Deer *et al.*, 1992); see inset for zoomed region. Al/(Al+Si) and Fe/(Fe+Mg) are on cation basis. (B) TiO_2 *vs.* Al_2O_3 (wt.%) diagram. Symbols as in Fig. 2.

biotite-bearing granites will be hereafter considered as a single suite (hereafter H-BG). Finally, two fine-grained samples plotting within the granite and alkaline granite fields are classified as aplite granite (AG). TMG and AG samples are slightly peraluminous, whereas H-BG rocks are metaluminous but plot close to the ASI [molecular $Al_2O_3/(CaO+K_2O+Na_2O)$] = 1 border line (Fig. 2B).

The TMG is a massive rock showing a medium-grained hypidiomorphic granular texture. In the central and southern parts of the pluton gradual transitions to more coarse-grained and porphyritic varieties with large K-feldspar crystals have been observed. These rocks are generally composed of quartz (~32 vol.%), K-feldspar (~34 vol.%), plagioclase (~25 vol.%), biotite (~5 vol.%), and muscovite (~3 vol.%) as main constituents, and apatite, zircon and opaques as accessories (total amount ~1 vol.%; Table 1). Quartz is anhedral and undulose, sometimes forming cataclastic vein-like aggregates. K-feldspar is microclinic and commonly encloses euhedral to anhedral plagioclase crystals. Muscovite occurs as large flakes and lath-shaped crystals, isolated or in clusters. Sometimes, they are intergrown with biotite. Few muscovites displaying subsolidus overgrowths are considered secondary in origin. H-BG are mainly hypidiomorphic medium-grained rocks consisting of quartz (~31 vol.%), K-feldspar (~30 vol.%), plagioclase (~29 vol.%), biotite (~8 vol.%), and amphibole (~3 vol.%), along with allanite, titanite, apatite, zircon and opaques as accessory minerals (total amount ~1 vol.%; Table 1). The AG are fine- to medium-grained rocks composed of quartz, K-feldspar, plagioclase, muscovite, and rare garnet and tourmaline.

Selected chemical microprobe analyses of feldspar, biotite, muscovite, amphibole, and garnet are presented in Table 2. K-feldspar exhibits a uniform composition in the TMG and H-BG groups with Or_{85}-Ab_{15} and Or_{95}-Ab_5, respectively. Plagioclase in the TMG is normally zoned and ranges in composition between An_{11} and An_{35}, and it does not show any evidence of crystallization under disequilibrium conditions. The H-BG rocks contain plagioclase with An_{17} to An_{34}. Although a majority of analyzed plagioclase grains shows a normal core-rim zoning, sieved textures and oscillatory variations of plagioclase composition interrupted by resorption zones have also been detected indicating crystallization under disequilibrium conditions. Most muscovites are characterized by relatively high TiO_2 contents, ranging 0.7–0.4 wt.%, and Mg/(Mg+Fe) (~0.5), favoring a primary origin (*e.g.* Miller *et al.*, 1981; Christofides *et al.*, 2007). The composition of biotites plot in the field of biotites as defined by Deer *et al.* (1992) (Fig. 3A), whereas biotites from TMG display higher Al_2O_3 and lower TiO_2 than those occurring in H-BG (Fig. 3B) as expected for such evolved rock compositions. Hornblende from a single H-BG sample (BK128) shows a magnesio-hornblende composition according to the classification of Leake *et al.* (1997), and is relatively poor in alumina and titanium (Table 2). Garnet with spessartine and almandine contents around 52 and 45 mol.% is restricted to the AG group. Their cores display slightly higher MnO and lower FeO contents than their rims.

Age

Eight new K/Ar age determinations on different mineral separates from granitoids of Mt. Bukulja are given in

Table 1. Modal compositions (Vol.%) of Bukulja granitoid rocks.

Sample	Rock type*	Q	K-F	Pl	Myr	Mu	Bt	Hbl	Ap	Zir	Aln	Tit	SM
BK128	H-BG	26.59	20.66	41.99	1.28	–	6.5	2.17	0.06	0.05	0.16	0.36	0.18
BK126	H-BG	29.82	30.44	30.75	0.71	–	7.95	–	0.04	0.02	0.03	0.16	0.08
BK121	H-BG	31.44	30.14	25.81	2.96	–	9.28	–	0.06	0.03	–	0.18	0.10
BK127	H-BG	32.29	28.63	30.14	0.62	–	7.04	–	0.03	0.03	–	–	0.14
BK114	TMG	29.52	20.71	22.29	1.25	0.85	24.62	–	0.43	0.03	–	–	0.18
BK118	TMG	32.81	26.65	30.25	2.06	1.24	6.75	–	0.05	0.04	–	–	0.15
BK109	TMG	37.42	19.18	28.75	1.77	5.25	7.39	–	0.06	0.02	–	–	0.16
BK125	TMG	34.48	24.82	28.35	2.17	2.43	7.53	–	0.06	0.04	–	–	0.12
BK111	TMG	31.48	24.63	32.24	2.81	2.16	6.50	–	0.04	0.01	–	–	0.13
BK107	TMG	36.44	25.31	26.84	1.02	2.80	7.45	–	0.02	0.03	–	–	0.09
BK123	TMG	32.90	26.14	31.66	1.55	1.42	5.93	–	0.11	0.04	–	0.12	0.13
BK124	TMG	32.13	27.42	30.49	1.03	2.96	5.64	–	0.05	0.03	–	0.08	0.17
BK117	TMG	28.34	28.16	32.86	2.3	3.86	4.31	–	0.02	0.03	–	–	0.12
BK106	TMG	33.23	26.83	27.05	0.47	5.37	6.78	–	0.04	0.02	–	–	0.21
BK101	TMG	33.41	26.44	30.04	1.02	1.86	6.97	–	0.05	0.04	–	–	0.17
BK102	TMG	29.69	32.28	26.56	1.75	5.65	3.98	–	0.02	0.01	–	–	0.06
BK122	TMG	33.16	25.18	31.98	1.82	1.51	6.12	–	0.05	0.02	–	0.10	0.06
BK112	TMG	31.22	25.81	31.86	1.85	4.92	4.21	–	0.04	0.02	–	–	0.07
BK115	TMG	33.28	25.73	31.55	2.53	2.25	4.56	–	0.02	0.01	–	–	0.07
BK119	TMG	30.18	28.65	28.62	2.48	6.22	3.67	–	0.06	0.02	–	–	0.10
BK116	TMG	32.85	28.75	27.23	1.12	5.38	4.37	–	0.04	0.04	–	–	0.22
BK104	TMG	33.62	27.53	27.12	1.81	3.95	5.83	–	0.04	0.03	–	–	0.07
BK103	TMG	31.52	28.68	26.73	2.88	4.69	5.35	–	0.06	0.01	–	–	0.08
BK105	TMG	32.08	26.60	27.96	1.83	4.92	6.45	–	0.03	0.05	–	–	0.08
BK110	TMG	35.21	23.80	25.80	1.52	4.33	9.10	–	0.04	0.02	–	–	0.18

*H-BG, Hornblende-biotite- and biotite-bearing granite; TMG, Two mica granite. Abbreviations: Aln – Allanite, Ap – Apatite, Bt – Biotite, Hbl – Hornblende, K-F – K-feldspar, Mu – Muscovite, Myr – Myrmekite, Pl – Plagioclase, Tit – Titanite, Q – Quartz, Zir – Zircon. SM – Secondary minerals: Chlorite, Sericite, Epidote. Samples are ordered by increasing silica contents.

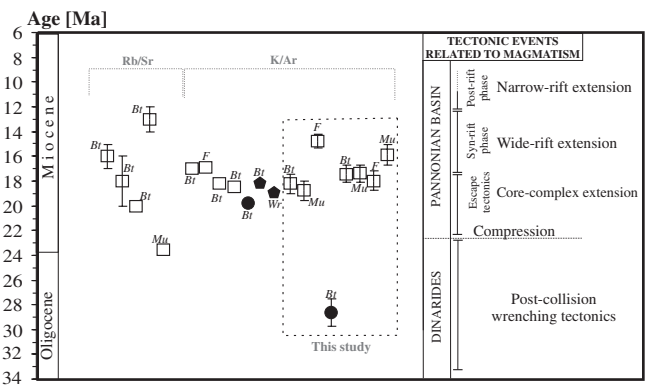

Fig. 4. Chart of Rb/Sr and K/Ar radiometric age determinations on minerals and whole-rock samples of the Mt. Bukulja granitoids and rocks from the contact aureole. The time distribution of major tectonic events related to magmatism in the Pannonian Basin and Dinarides is given at the right-hand side (*e.g.* Cvetković *et al*., 2004b). Symbols as in Fig. 2, and solid pentagons for contact-metamorphic rocks. Bt – biotite, F – feldspar, Mu – Muscovite, Wr – Whole-rock. Vertical bars represent the uncertainties. Data inside the box with dashed lines are from this work. Previous data for Mt. Bukulja rocks after Deleon (1969), Divljan & Cvetić (1991), and Karamata (unpublished).

Table 3. New and old K/Ar and Rb/Sr radiometric ages are summarized and shown as a chart in Fig. 4 along with time distribution of major Oligocene and Miocene tectonic events in the Pannonian Basin and Dinarides.

New K/Ar ages for the TMG (18.8–17.4 Ma) are well within the range of the earlier age determinations on Mt. Bukulja rocks, except for a feldspar separate, which gave an age of 14.8 Ma. Most age determinations, whatever the method, fall in an age range between 20 Ma and 16 Ma, including those obtained on two samples from the contact aureole. Muscovite fractions from an aplitic granite sample gave an age of 15.9 Ma, corresponding to the lower end of the range for the TMG. A previous K/Ar age on biotite from a biotite-bearing sample reveals an age of 19.8 Ma (Deleon, 1969), similar to the TMG ages (within the error limits), whereas our new biotite age on a similar sample gave an older age (28.6 Ma) well outside the age field of the TMG.

In summary, the range between 20 Ma and 17 Ma can be regarded as the emplacement age of the TMG and thus the intrusion age of the bulk granitoid body of Mt. Bukulja. The age of the H-BG group remains poorly constrained because the earlier and new data gave conflicting results.

Geochemistry

Major and trace elements data including REE concentrations of 33 granitoid samples, three BLD rocks, and three samples from the metamorphic basement are given in Tables 4 and 5, whereas Sr-Nd isotope analyses are presented

Table 2. Representative microprobe analyses of minerals present in Mt. Bukulja granitoids.

	K-feldspar								Plagioclase							
Rock type*	H-GB				TMG			AG	H-GB				TMG			AG
Sample	BK128	BK126	BK114	BK101	BK103	BK105	BK109	BK113	BK128	BK126	BK114	BK101	BK103	BK105	BK107	BK113
	core	rim	core	core	core	core	rim	core	core	rim	rim	core	rim	core	core	core
SiO_2	65.27	65.29	65.14	66.17	66.34	65.97	66.35	65.05	58.94	61.08	61.73	61.74	62.59	63.54	61.59	66.00
Al_2O_3	18.92	19.06	19.13	18.54	18.5	18.39	18.41	19.19	26.33	24.52	23.44	23.79	23.13	22.73	24.19	20.68
CaO	-	0.07	-	-	0.06	0.12	-	-	7.39	5.27	4.57	5.30	4.45	4.23	5.13	0.91
Na_2O	0.7	1.77	1.12	1.34	1.44	1.13	2.06	1.23	7.83	9.36	9.91	8.71	9.32	9.78	9.37	12.07
K_2O	15.1	13.71	14.29	14.29	13.8	14.2	13.35	14.47	-	0.33	0.22	0.24	0.12	0.04	0.21	0.13
sum	99.99	99.83	99.68	100.34	100.08	99.69	100.17	99.94	100.49	100.56	99.87	99.78	99.61	100.32	100.49	99.79
Ab	6.58	16.40	10.64	12.47	13.69	10.79	19.00	11.44	65.72	74.94	78.77	73.83	78.60	80.53	75.91	95.35
An	-	-	-	-	-	-	-	-	34.28	23.32	20.07	24.83	20.74	19.25	22.97	3.97
Or	93.42	83.60	89.36	87.53	86.31	89.21	81.00	88.56	-	1.74	1.15	1.34	0.67	0.22	1.12	0.68

	Biotite								Muscovite				Amphibole		Garnet	
Rock type*	H-GB				TMG				TMG			AG	H-BG		AG	
Sample	BK128	BK126	BK114	BK101	BK103	BK105	BK107	BK112	BK114	BK101	BK103	BK113	BK128	BK128	BK113	BK113
	core	rim	core	core	core	rim	rim	rim	core	core	rim	core	core	rim	core	rim
SiO_2	37.25	36.43	36.05	36.8	36.94	36.27	35.5	37.28	45.47	46.71	47.04	45.93	49.48	50.44	35.02	35.66
TiO_2	3.75	3.16	3.18	2.74	2.91	2.64	2.83	2.84	1.03	1.37	1.02	-	0.42	0.20	-	-
Al_2O_3	14.98	16.6	19.02	18.41	19.21	20	19.22	19.06	35.26	33.83	33.8	35.69	4.75	3.41	20.28	20.32
FeO	23.09	21.65	20.84	20.16	20.98	23.19	23.76	20.93	1.53	1.56	1.94	2.21	19.92	19.32	24.80	26.93
MnO	0.73	0.73	-	0.42	0.39	0.59	-	0.57	-	0.04	0.18	-	0.80	0.94	19.33	16.53
MgO	8.3	8.5	7.61	8.51	6.63	4.74	5.73	6.29	0.92	0.85	0.85	-	9.94	10.90	0.30	0.26
CaO	-	-	-	-	-	-	-	-	-	-	0.04	-	11.89	12.36	0.33	0.43
Na_2O	0.43	0.41	-	0.24	0.14	0.09	0.39	-	0.69	0.35	0.43	0.47	0.99	0.77	-	-
K_2O	8.87	8.68	9.25	8.99	8.98	9.16	9.17	9.11	10.22	10.08	10.06	10.39	0.41	0.17	-	-
Sum	97.4	96.16	95.95	96.27	96.18	96.68	96.6	96.08	95.12	94.79	95.36	94.69	98.60	98.51	100.06	100.13
Si	5.652	5.555	5.463	5.540	5.572	5.512	5.428	5.629	6.075	6.241	6.261	6.166	7.347	7.467	5.845	5.918
Al IV	2.348	2.445	2.537	2.460	2.428	2.488	2.572	2.371	1.925	1.759	1.739	1.834	0.653	0.533	3.989	3.974
AlVI	0.330	0.538	0.860	0.806	0.988	1.095	0.892	1.021	3.627	3.568	3.563	3.812	0.179	0.062	-	-
Ti	0.428	0.362	0.362	0.310	0.330	0.302	0.325	0.322	0.103	0.138	0.102	-	0.047	0.022	-	-
Fe^{3+}	-	-	-	-	-	-	-	-	-	-	-	-	0.235	0.252	3.461	3.737
Fe^{2+}	2.930	2.761	2.641	2.538	2.647	2.947	3.038	2.643	0.171	0.174	0.216	0.248	2.239	2.140	-	-
Mn	0.094	0.094	-	0.054	0.050	0.076	-	0.073	-	0.005	0.020	-	0.101	0.118	2.732	2.323
Mg	1.877	1.932	1.719	1.910	1.491	1.074	1.306	1.416	0.183	0.169	0.169	-	2.200	2.406	0.075	0.064
Ca	-	-	-	-	-	-	-	-	-	-	0.006	-	1.892	1.960	0.059	0.076
Na	0.126	0.121	-	0.070	0.041	0.027	0.116	-	0.179	0.091	0.111	0.122	0.285	0.221	-	-
K	1.717	1.688	1.788	1.727	1.728	1.776	1.789	1.755	1.742	1.718	1.708	1.779	0.078	0.032	-	-
Mg#	0.383	0.404	0.394	0.424	0.356	0.262	0.301	0.343	0.517	0.486	0.417	-	0.496	0.529	-	-

*H-BG, Hornblende-biotite- and biotite-bearing granite; TMG, Two-mica granite; AG, Aplite granite.
The whole set of microprobe data is available upon request to the corresponding author.

Table 3. New K/Ar ages of Mt. Bukulja granitoid rocks.

Sample	Rock type*	Dated Fraction	K_2O%	^{40}Ar rad (%)	^{40}Ar rad (ccSTP/g)	K/Ar (Ma)
2170	TMG	biotite	6.85	45.9	4.865×10^{-6}	18.2 ± 0.8
2170/1	TMG	muscovite	7.71	52.2	5.649×10^{-6}	18.8 ± 0.8
2170/2	TMG	feldspar	3.99	67	2.305×10^{-6}	14.8 ± 0.6
4068	TMG	biotite	6.95	55.9	4.744×10^{-6}	17.4 ± 0.7
4068/1	TMG	muscovite	5.38	71.6	3.656×10^{-6}	17.4 ± 0.7
4068/2	TMG	feldspar	2.63	53.5	1.845×10^{-6}	18.9 ± 0.8
4067	BG	biotite	5.91	82.8	6.625×10^{-6}	28 ± 1.1
3938	AG	muscovite	7.79	31.2	4.826×10^{-6}	15.8 ± 0.8

*H-BG, Hornblende-biotite- and biotite-bearing granite; TMG, Two mica granite; AG, Aplite granite.

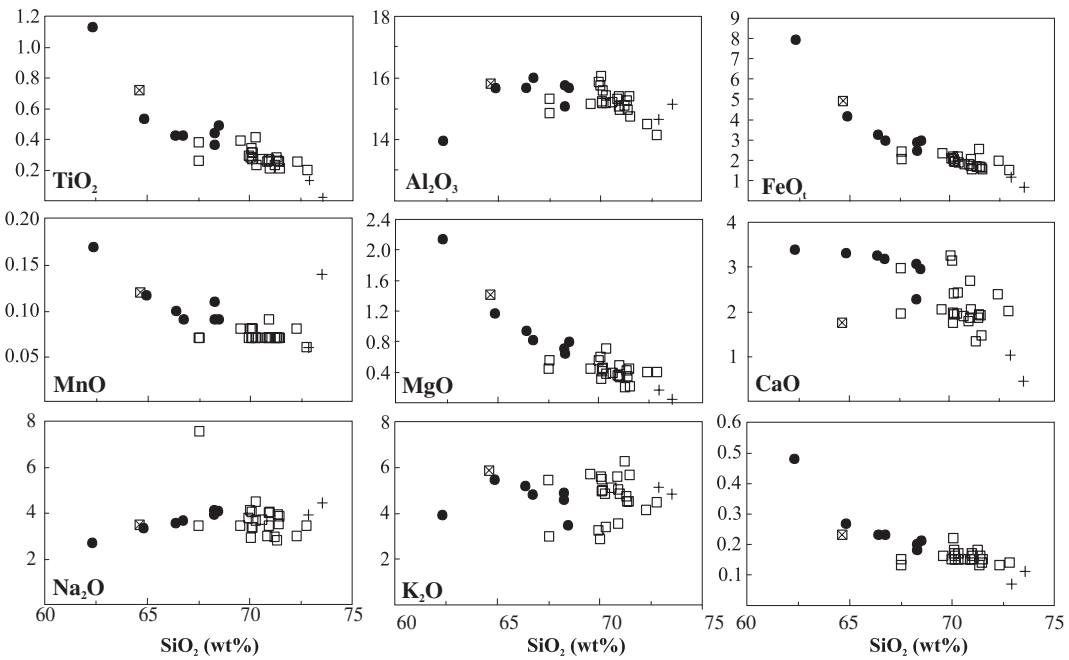

Fig. 5. Selected major elements (wt.%) variation diagrams for Mt. Bukulja granitoid rocks. Symbols as in Fig. 2, and square with '×' is for sample BK114 considered to have evidence of biotite cumulus.

in Table 6. The Sr and Nd initial isotope ratios were calculated for an age of 20 Ma. The chemical compositions of three BLD and three samples of adjacent metamorphic rocks are given in order to constrain possible mantle/derived basic melts and local upper crustal characteristics.

Details upon the analytical methods used in this paper are given in the Appendix.

Major and trace elements

TMG samples span an overall silica range of 67.5–72.8 wt.% with one exception (BK114; SiO_2 = 64.65 wt.%). This sample contains, however, a very high amount of modal biotite (~24 vol.%) with Al_2O_3 and TiO_2 contents similar to biotites from TMG samples (Table 2 and Fig. 3), and it has anomalous contents of Rb (Table 4). All these features may have resulted from cumulus of biotite. H-BG whole-rock samples show slightly lower SiO_2 contents, ranging from 62 to 68 wt.%.

The two granitoid groups show negative trends for most major oxides with increasing silica contents (Fig. 5). Na_2O displays a positive correlation trend in H-BG, and scattering in TMG, whereas CaO and K_2O contents scatter for both suites. In keeping with major element variations, most trace element contents decrease with increasing SiO_2 wt.%, with some scattering evident mainly in TMG (Fig. 6). Sr and Ba have a bell-shaped variation pattern in H-BG and quite uniform contents in TMG. Rb and Pb have a uniform pattern for the two groups of rocks. TMG samples show larger scattering, which is especially evident for Cr, Th, La and Ce concentrations. On primitive mantle-normalized trace element diagrams (Fig. 7A and B) all the granitoid groups show similar variations with negative anomalies at Ba, Nb, Ta and Ti, as well as with a distinctive positive

Table 4. Representative major (wt.%) and trace element (ppm) analyses of Bukulja granitoids, BLD, and MB rocks.

Rock type*	H-BG												TMG										
Sample	Bk128	BK120	BK133	BK132	BK126	BK121	BK127	BK114	BK118	BK109	BK125	BK111	BK129	BK107	BK123	BK124	BK117	BK106	BK101	BK102	BK122	BK112
SiO_2	64.85	62.34	66.40	66.75	68.28	68.29	68.49	64.65	67.52	67.54	69.55	69.96	70.04	70.08	70.11	70.12	70.14	70.3	70.32	70.61	70.87	70.94
TiO_2	0.55	1.13	0.42	0.42	0.44	0.36	0.49	0.72	0.38	0.26	0.39	0.29	0.28	0.34	0.31	0.31	0.27	0.41	0.23	0.27	0.25	0.27
Al_2O_3	15.76	13.95	15.68	16.01	15.07	15.76	15.66	15.80	14.84	15.31	15.15	15.85	15.74	16.06	15.23	15.18	15.6	15.17	15.43	15.21	15.32	15.41
Fe_2O_3	2.12	5.00	2.55	2.79	2.16	1.65	1.92	2.69	1.97	1.82	2.09	2.04	2.24	1.87	1.46	1.42	1.78	2	1.82	1.63	1.87	1.5
FeO	2.30	3.41	0.96	0.42	0.91	0.96	1.21	2.33	0.45	0.23	0.45	0.23	0.12	0.26	0.72	0.62	0.29	0.35	0.21	0.33	0.09	0.37
MnO	0.12	0.17	0.10	0.09	0.11	0.09	0.09	0.12	0.07	0.07	0.08	0.07	0.08	0.07	0.08	0.07	0.08	0.07	0.07	0.07	0.07	0.07
MgO	1.18	2.14	0.94	0.82	0.71	0.64	0.79	1.41	0.44	0.55	0.44	0.55	0.6	0.31	0.41	0.44	0.45	0.37	0.7	0.39	0.35	0.34
CaO	3.33	3.38	3.25	3.18	3.06	2.28	2.95	1.75	1.95	2.97	2.04	t4 3.25	3.14	1.75	1.98	1.93	2.4	1.95	2.43	1.9	1.79	1.85
Na_2O	3.24	2.68	3.54	3.65	3.92	4.12	4.08	3.46	3.45	7.57	3.45	3.79	4.1	2.9	3.35	4.05	3.35	3.68	4.47	3.71	3	3.45
K_2O	5.48	3.89	5.16	4.81	4.58	4.88	3.45	5.84	5.45	2.97	5.71	3.25	2.85	5.6	5.47	4.95	4.97	4.83	3.37	5.11	5.57	5.03
P_2O_5	0.27	0.48	0.23	0.23	0.20	0.18	0.21	0.23	0.15	0.13	0.16	0.15	0.22	0.18	0.17	0.15	0.16	0.17	0.15	0.15	0.15	0.15
LOI	0.79	1.43	0.77	0.83	0.55	0.79	0.65	1.00	3.33	0.57	0.49	0.57	0.58	0.57	0.71	0.77	0.51	0.7	0.79	0.62	0.67	0.62
V	46	93	32	33	25	14	25	52	6	12	6	12	18	6	6	7	6	6	6	6	6	6
Cr	29	49	20	25	21	23	19	28	19	12	19	12	11	10	13	16	13	6	19	11	14	15
Co	7	16	6	< 5	< 5	< 5	6	7	< 5	< 5	< 5	< 5	< 5	< 5	< 5	t4 < 5	< 5	< 5	< 5	< 5	< 5	< 5
Ni	16	30	11	12	14	14	10	21	11	8	11	8	7	13	13	11	16	15	10	13	12	13
Ga	22	22	24	22	21	17	25	28	24	18	24	18	26	20	18	21	18	23	19	17	17	22
Rb	200	307	186	178	223	310	211	463	287	153	287	153	189	312	307	293	287	291	183	308	313	291
Sr	474	368	493	502	381	324	316	108	148	214	148	214	221	150	169	152	173	161	205	154	156	132
Y	27	44	18	20	14	15	13	17	9	9	9	9	7	8	12	7	8	9	8	8	11	10
Zr	188	344	198	196	133	124	198	151	155	116	155	116	129	147	124	137	103	202	118	111	118	106
Nb	15	34	15	13	11	18	10	19	8	< 5	8	< 5	8	11	7	8	9	11	< 5	7	8	7
Ba	766	589	743	721	542	612	473	311	420	343	420	343	265	415	419	351	348	505	356	384	382	291
La	50	32	44	53	32	21	30	34	31	23	31	23	22	36	29	30	19	32	24	28	23	15
Pb	59	28	49	42	40	45	36	37	50	28	50	28	36	53	48	47	43	45	29	43	47	39
Ce	74	67	49	74	28	12	66	39	47	8	47	8	25	33	41	47	17	65	21	9	49	12
Th	25	24	25	28	21	29	26	24	30	11	30	11	18	22	23	26	16	24	10	14	21	18

Table 4. (Cont.)

Rock type*	TMG									AG		BLD		MB			
Sample	BK115	BK119	BK116	BK104	BK103	BK131	BK105	BK110	BK13	BK108	BK113	AR99/2**	Ar99/4**	BK100	BK134	BK135	BK136
SiO_2	70.94	70.99	71.23	71.32	71.37	71.43	71.47	72.3	72.79	72.87	73.53	42.39	44.38	42.41	74.62	79.69	60.74
TiO_2	0.26	0.21	0.23	0.28	0.26	0.25	0.21	0.25	0.2	0.13	0.02	0.79	0.81	1.10	0.64	0.18	1.37
Al_2O_3	15.07	14.96	15.09	15.26	14.96	15.39	14.75	14.48	14.13	14.65	15.16	10.21	10.28	9.12	12.93	11.04	14.78
Fe_2O_3	2.07	1.37	1.54	2.02	1.44	1.71	1.41	1.53	1.43	1.16	0.56	7.57	9.33	7.00	3.47	1.03	9.23
FeO	0.19	0.29	0.28	0.55	0.37	0.08	0.25	0.57	0.22	0.11	0.16	-	-	3.98	0.64	0.07	
MnO	0.09	0.07	0.07	0.07	0.07	0.07	0.07	0.08	0.06	0.06	0.14	0.12	0.13	0.18	0.08	0.05	0.13
MgO	0.48	0.33	0.2	0.42	0.34	0.44	0.21	0.40	0.40	0.17	0.04	10.05	12.6	11.31	1.05	0.12	1.59
CaO	2.68	2.04	1.33	1.86	1.93	1.91	1.47	2.39	2.01	1.03	0.46	9.54	8.18	9.11	1.00	0.23	0.36
Na_2O	3.99	4.02	2.95	2.80	3.93	3.53	3.86	2.99	3.43	3.92	4.44	1.28	0.39	4.38	1.64	2.34	1.55
K_2O	3.53	4.82	6.24	4.72	4.51	4.49	5.66	4.14	4.45	5.12	4.84	3.06	5.93	5.21	2.14	4.2	5.51
P_2O_5	0.17	0.16	0.18	0.13	0.16	0.14	0.15	0.13	0.14	0.07	0.11	0.96	1.02	1.01	0.11	0.06	0.14
LOI	0.53	0.74	0.65	0.74	0.67	0.56	0.49	0.74	0.74	0.71	0.55	11.07	6.25	5.18	1.70	0.98	3.50
V	13	6	6	9	6	15	6	6	13	6	6	159	188	187	60	13	101
Cr	22	13	16	16	11	5	12	17	11	11	< 5	824	1124	958	50	6	82
Co	< 5	< 5	< 5	< 5	< 5	< 5	< 5	< 5	< 5	< 5	< 5	42	53	44	8	< 5	10
Ni	14	12	13	14	10	12	17	17	11	15	15	275	392	284	25	12	40
Ga	22	20	24	23	20	22	21	23	20	20	23	10	17	12	16	10	35
Rb	216	281	360	291	258	285	335	248	224	293	453	148	236	235	120	187	210
Sr	173	130	89	145	152	190	109	157	162	39	11	516	516	869	157	118	59
Y	9	9	7	10	10	13	8	12	9	17	7	25	29	23	20	15	50
Zr	108	96	99	123	111	125	93	99	99	58	24	202	197	255	182	94	276
Nb	8	8	8	11	8	10	9	10	5	16	13	12	11	13	10	10	21
Ba	230	289	272	305	329	344	262	285	312	63	4	1276	2634	2005	411	204	530
La	28	16	30	26	34	39	31	21	26	21	9	-	-	33	26	27	47
Pb	32	40	47	47	51	48	50	44	44	52	23	33	7	19	30	40	42
Ce	12	20	36	25	13	24	31	10	10	< 5	< 5	-	-	52	22	37	119
Th	16	14	29	20	20	19	26	15	16	15	< 5	-	-	22	11	30	25

* H-BG, Hornblende-biotite- and biotite-bearing granite; TMG, Two-mica granite: AG, Aplite granite; BLD, Bukulja lamprophyric dyke; MB, Metamorphic basement.
** Data from Prelević *et al.* (2005).
- Not determined.

Table 5. Rare earth element and trace element contents for representative Bukulja granitoids, BLD, and MB rocks.

Sample	Rock type*	La	Ce	Nd	Sm	Eu	Tb	Yb	Lu	Th	U	Cs	Hf	Ta	Cr	Sc	Co
BK128	H-BG	61	104	41	8.2	1.4	0.7	2.2	0.3	32	8.7	9	5.7	1.2	17	6.8	5
BK133	H-BG	40	76	30	6.4	1.4	0.8	2	0.2	22	6.7	10	5.2	1.1	11	5.1	4.1
BK121	H-BG	30	54	21	4.5	0.9	0.5	1.6	0.2	21	11	43	3.7	2.3	18	3.3	3
BK127	H-BG	45	78	28	5.1	1	0.5	0.9	0.1	22	9	23	4.9	1.1	22	3.7	3.6
BK111	TMG	21	36	15	3	0.6	0.3	0.7	0.1	9.5	1.9	7	3.3	0.7	4.9	2.7	2.3
BK107	TMG	34	59	25	4.9	0.7	0.3	0.7	0.1	18	3.5	23	4	1.4	10	1.9	1.6
BK124	TMG	33	61	20	4.4	0.7	0.5	0.8	0.1	19	11	17	3.6	0.9	15	2.3	1.9
BK112	TMG	24	45	15	3.1	0.6	0.3	0.8	0.1	13	3.3	13	3	1.2	13	2.3	1.7
BK115	TMG	21	36	14	3.1	0.5	0.3	0.8	0.1	12	2.6	25	3.2	2.2	15	2.9	2.3
BK119	TMG	17	36	15	3.1	0.6	0.4	0.8	0.1	11	2.9	12	2.6	0.9	14	1.9	1.5
BK116	TMG	33	59	24	4.1	0.5	0.4	0.5	0.1	20	3.4	19	3	1	10	1.4	1.1
BK105	TMG	32	59	26	5.2	0.5	0.4	0.7	0.1	23	7.5	23	3.2	1.5	13	1.4	1.4
BK130	TMG	19	33	16	2.9	0.5	0.4	0.7	0.1	11	2.6	18	2.6	1	4.8	2.1	1.4
AR99/2**	BLD	29	60	32	6.5	2	0.7	1.6	0.2	15.9	6.1	10.3	4.5	-	-	26	-
AR99/4**	BLD	33	69	36	7.5	3.1	0.9	1.7	0.3	18.4	6.4	20.2	5.2	-	-	28	-
BK134	MB	24	47	18	4.1	0.9	0.6	2	0.3	7.7	2.3	13	4.6	0.8	39	8.6	7.1
BK136	MB	40	78	32	6.9	1.3	0.9	3.1	0.5	15	3.8	8	5.8	1.2	64	13	7

* H-BG, Hornblende-biotite- and biotite-bearing granite; TMG, Two-mica granite: BLD, Bukulja lamprophyric dyke; MB, Metamorphic basement.
** Data from Prelević *et al*. (2005).

spike at Pb. In comparison with the TMG, H-BG samples show slightly higher overall trace element concentrations characterized by higher ΣREE, slightly lower extent of REE fractionation, and a slightly lower negative Eu-anomaly on chondrite-normalized REE diagrams (Fig. 7B). Overall, Mt. Bukulja granitoid rocks have generally similar trace element and REE patterns to Early/Middle Miocene acid volcanics of the northern Pannonian Basin (Fig. 7).

Sr-Nd isotopes

The $^{143}Nd/^{144}Nd_i$ *vs.* $^{87}Sr/^{86}Sr_i$ diagram is presented in Fig. 8. The isotope ratios from the studied granitoid rocks form a trend of increasing radiogenic strontium and decreasing radiogenic neodymium, and occupy a field between 0.7065 and 0.7137 for $^{87}Sr/^{86}Sr_i$, and 0.51265 and 0.51230 for $^{143}Nd/^{144}Nd_i$. A generally similar Sr-Nd isotopic pattern is displayed by coeval (20–15 Ma) rhyolite and rhyodacite volcanics from the Pannonian Basin (Fig. 8, field 1). Furthermore, Sr-Nd isotope ratios of the Mt. Bukulja granitoids overlap with the field of Tertiary primitive minettes of Serbia (Fig. 8, field 2). This field extends further to more primitive isotopic compositions approaching the field of asthenospheric-derived East Serbian alkaline basalts (Fig. 8, field 3). The trend of the most evolved Mt. Bukulja rocks points towards the isotopic composition of the samples from the intruded metamorphic basement (Fig. 8).

Discussion

Products of the Mt. Bukulja plutonism can be divided into two main magmatic groups, H-BG and TMG, on the basis of their mineralogical assemblage and ASI: presence of primary muscovite and ASI higher than 1 in TMG, the opposite holds for H-BG. The two groups have also different degree of evolution and their relative percentage in outcrops is about 95 % and 5 %, respectively. The contacts between the rocks of the two groups are hidden by thick soil cover, and the available age data are not conclusive regarding the sequence of emplacement of TMG and H-BG.

TMG and H-BG groups have many other differences. TMG biotites show higher Al_2O_3 values in comparison to biotites from H-BG rocks (Fig. 3B). Despite the low number of analysed samples, mainly for the H-BG group, the Sr and Nd isotopic ratios in the TMG group can be considered much more variable than in the H-BG one (Table 6). Petrographic characteristics of H-BG are consistent with a genesis in which magma interaction processes played a major role, as indicated by disequilibrium phenomena in plagioclase (*e.g.* Hibbard, 1995; Pietranik *et al*., 2006). By contrast, evidence of disequilibrium processes in minerals is lacking in TMG. These rocks, in fact, display neither macroscopic, such as the presence of microgranular enclaves (*e.g.* Didier & Barbarin, 1991; Perugini *et al*., 2003), nor microscopic evidence that may indicate magma mixing processes.

In Fig. 9 the TMG samples show a distinctive positive correlation between the $^{87}Sr/^{86}Sr_i$ values and Rb/Sr ratios and K_2O contents. By contrast, the H-BG rocks exhibit no correlation between Sr isotope and Rb/Sr ratios as well as between Sr isotope ratios and K_2O contents. The positive correlation between $^{87}Sr/^{86}Sr_i$ and Rb/Sr shown by the TMG samples cannot be explained by variable abundances of initial ^{87}Rb. The alignment cannot be considered an isochron because the calculated age (58 ± 18) has no geochronological significance, and because MSWD (Mean Square of Weighted Deviations) is greater than 5.5. Thus, the TMG series has to be regarded as having been affected by open system processes. In addition, the TMG

Table 6. Sr and Nd isotopic compositions of representative Bukulja granitoids, BLD, and MB rocks.

Sample	Rock type*	Rb	Sr	$^{87}Rb/^{86}Sr$	2σ	$(^{87}Sr/^{86}Sr)_m$	2σ	$(^{87}Sr/^{86}Sr)_{20}$	2σ	Sm	Nd	$^{147}Sm/^{144}Nd$	2σ	$^{143}Nd/^{144}Nd$	2σ	$(^{143}Nd/^{144}Nd)_{20}$	2σ
BK128	H-BG	200	474	1.22	9	0.708161	9	0.70781	3	8.2	41	0.57	3	0.51250	4	0.51243	4
BK133	H-BG	186	493	1.09	9	0.708076	18	0.70777	3	6.4	30	0.6	4	0.51262	5	0.51255	5
BK121	H-BG	310	324	2.7	2	0.708565	9	0.70778	6	4.5	21	0.61	4	0.51264	4	0.51256	4
BK127	H-BG	211	316	1.9	1	0.708229	15	0.70768	5	5.1	28	0.51	3	0.51249	5	0.51242	5
BK105	TMG	335	109	8.9	7	0.714491	27	0.71196	20	5.2	26	0.58	3	0.51233	5	0.51225	5
BK107	TMG	312	150	6	5	0.712682	16	0.71097	14	4.9	25	0.56	3	0.51233	3	0.51226	3
BK111	TMG	153	214	2.1	2	0.707105	12	0.70652	5	3.0	15	0.58	3	0.51249	4	0.51241	4
BK112	TMG	291	132	6.4	5	0.712560	22	0.71075	15	-	-	-	-	-	-	-	-
BK115	TMG	216	173	3.6	3	0.708717	7	0.70769	8	3.1	14	0.63	4	0.51260	5	0.51252	5
BK116	TMG	360	89	11.7	9	0.717012	31	0.71368	26	4.1	24	0.48	3	0.51229	2	0.51223	2
BK119	TMG	281	130	6.3	5	0.712256	1	0.71048	15	3.1	15	0.59	4	0.51245	5	0.51237	5
BK124	TMG	293	152	5.6	4	0.712676	9	0.71109	13	-	-	-	-	-	-	-	-
BK130	TMG	224	162	4	3	0.709633	4	0.70850	10	2.9	16	0.52	3	0.51241	3	0.51235	3
AR99/2**	BLD	148	513	¡	¡	0.707760	11	0.70745	#	6.46	31.96	-	-	0.512536	5	0.51252	-
BK134	MB	120	157	2.2	2	0.721358	4	0.72073	7	4.1	18	0.63	4	0.51213	4	0.51205	4
BK136	MB	210	59	10.3	8	0.734391	2	0.73146	23	6.9	32	0.61	4	0.51204	6	0.51196	6

*H-BG, Hornblende-biotite- and biotite-bearing granite; TMG, Two-mica granite: BLD, Bukulja lamprophyric dyke; MB, Metamorphic basement.
Rb, Sr, and Sm, Nd analysed by XRF and INAA, respectively. Quoted errors refer to the last digit.
**Data from Prelević *et al*. (2005); initial ratios calculated at 23 Ma; # not reported.
- not determined

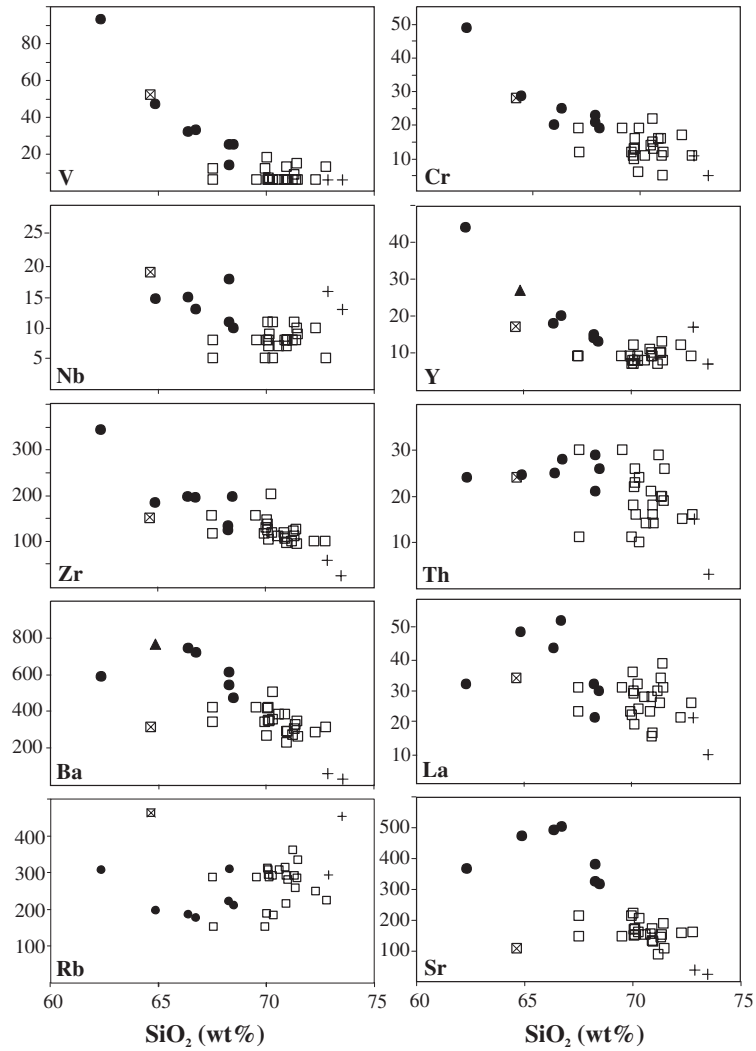

Fig. 6. Selected trace element (ppm) variation diagrams for Mt. Bukulja granitoid rocks. La and Ce determined by XRF analyses. Symbols as in Fig. 2 and 5.

have a similar range of $^{87}Sr/^{86}Sr_i$ as the Tertiary primitive minettes of Serbia (Prelević *et al*., 2005), whereas the H-BG group points to the isotopic composition of the Bukulja lamprophyric dyke. The same holds for $^{143}Nd/^{144}Nd$ values, though with more scattering, implying a possible genetic link between the H-BG and BLD. Above considerations suggest that the TMG and H-BG groups derived from different processes that will be discussed separately in the following section.

Origin and evolution of H-BG

H-BG rocks exhibit a low variability (2 on the fourth decimal) of initial Sr isotope ratios despite the variable Rb/Sr and K_2O contents. As a first approximation, a closed system process can be supposed to explain the geochemical variability within the H-BG rocks. To test such a hypothesis we utilized the MELTS software (Ghiorso & Sack, 1995; Asimow & Ghiorso, 1998; Smith & Asimow, 2005) to model a possible crystallization sequence of a lamprophyric melt having the BLD composition. The choice of such parental magma is dictated by the composition of biotites (Fig. 3) and by isotopic composition (Fig. 9). We started the crystallization using the liquidus temperature calculated by the software (*ca*. 1279 °C), varying the oxygen fugacities and assuming pressures below 5.0 kbar as suggested by the presence of olivine as phenocryst phase in all the primitive minettes of Serbia (Prelević *et al*., 2005). The composition of calculated residual liquids after fractional crystallization does not approach compositions of the H-BG rocks under any condition of oxygen buffer and pressure below 5.0 kbar. This suggests that the H-BG rocks could not have derived from a BLD-like magma by a closed system process.

A hypothesis invoking evolution as an open system is more plausible because: i) petrographic features suggestive of magma mixing do exist in the H-BG rocks, and ii) H-BG rocks have Sr isotopic composition approaching the field of Serbian primitive minettes; in particular, $^{87}Sr/^{86}Sr$ values are almost identical to those of BLD (Fig. 9).

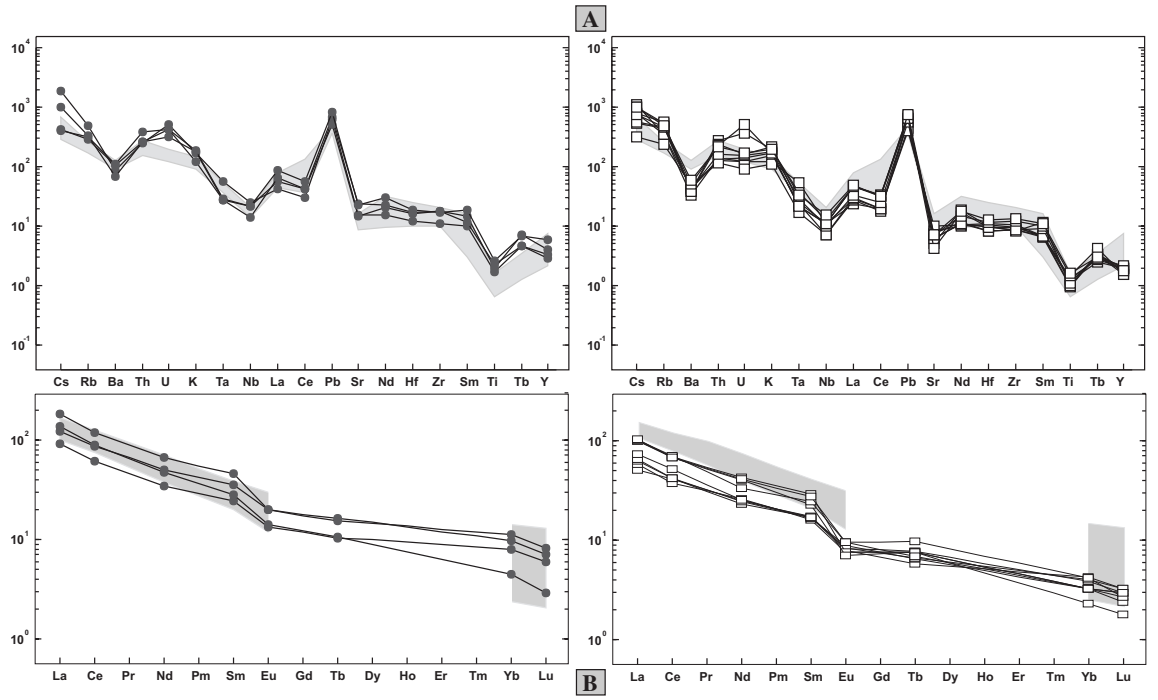

Fig. 7. Multielement spiderdiagrams for H-BG and TMG normalized to a primitive mantle (A, B), and chondrite-normalized REE diagram (C, D). The patterns of Early/Middle Miocene acid volcanic rocks of the northern Pannonian Basin (NPB) are also shown (grey area; Harangi *et al*., 2001; Seghedi *et al*., 2004). Normalization values for primordial mantle and REE according to McDonough *et al*. (1992) and Haskin *et al*. (1966), respectively. Symbols as in Fig. 2.

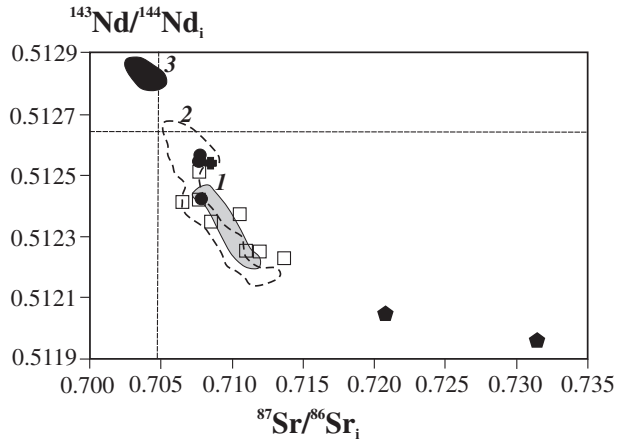

Fig. 8. $^{143}Nd/^{144}Nd_i$ *vs.* $^{87}Sr/^{86}Sr_i$ variation diagram for Mt. Bukulja granitoid rocks. Sr-Nd isotopic compositions are also shown for: 1. Early/Middle Miocene acid volcanics of the Northern Pannonian Basin (Harangi *et al*., 2001; Seghedi *et al*., 2004); 2. Tertiary calc-alkaline and potassic/ultrapotassic volcanic rocks of Serbia (Cvetković *et al*., 2004b; Prelević *et al*., 2005); 3. East Serbian Palaeocene/Eocene mafic alkaline rocks (Cvetković *et al*., 2004b). Symbols as in Fig. 2, plus greek cross for Bukulja lamprophyric dyke, and pentagons for basement rocks (MB) outcropping in the surrounding of the Bukulja pluton.

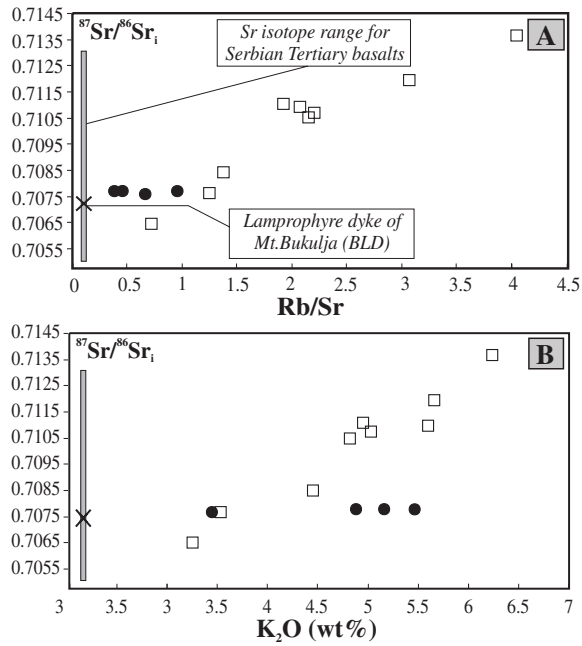

Fig. 9. Diagrams of covariation between $^{87}Sr/^{86}Sr_i$ and Rb/Sr (A) and K_2O wt.% (B). Data for Serbian Tertiary basalts and BLD are from: Prelević *et al*. (2005); Cvetković *et al*. (2004b). Symbols as in Fig. 2.

Interaction processes can be tested by a Mixing plus Fractional Crystallization (MFC) model, with an analogous mathematical formulation as used for the Assimilation plus Fractional Crystallization (AFC) process by De Paolo (1981). The restricted member of samples from the H-BG group, due to the small outcropping area, prevents a

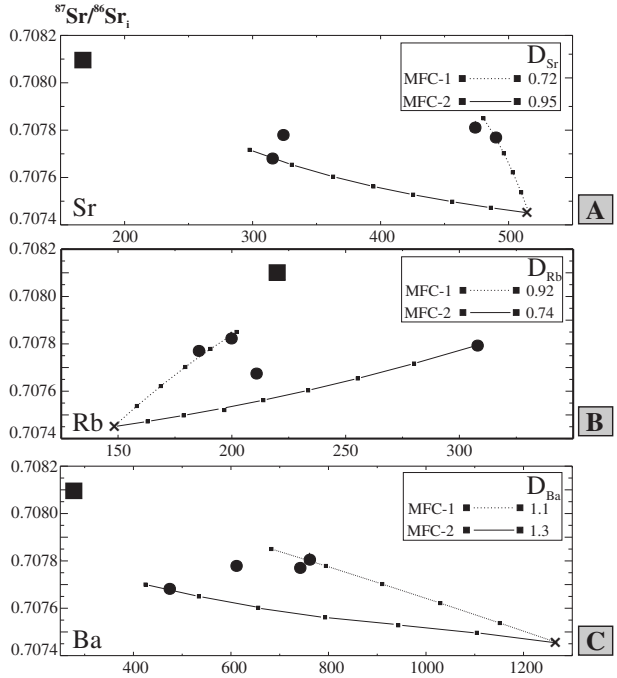

Fig. 10. Diagrams showing results of MFC modeling for H-BG rocks. Two MFC lines are needed to encompass the variability of composition of the rocks. Modelled bulk partition coefficients D for Sr, Rb, and Ba are also given. Cross-parental end-member (Bukulja lamprophyric dyke composition); solid square-average composition of TMG samples plotting at the end of the $^{87}Sr/^{86}Sr$ *vs.* Rb/Sr trend defined by the H-BG group in Fig. 9; tick marks are reported at 10% intervals of crystal fractionation. Other symbols as in Fig. 2. For further explanations see text.

complete modeling of the genesis and evolution of these rocks. However, some aspects can be highlighted by testing the hypothesis whether the H-BG rocks may have derived by MFC processes between BLD and TMG. The average composition of the TMG samples plotting at the end of the $^{87}Sr/^{86}Sr$ *vs.* Rb/Sr trend defined by the H-BG group in Fig. 9 have been used as acid end-member. In the TMG group there is no evidence of significant interaction between mafic and felsic magmas, and the outcropping of mafic granitoids is very restricted in Mt. Bukulja. It seems reasonable, hence, to use a limited batch of TMG as acid end-member in the interaction process with BLD magma. The results of the modeling are presented in Fig. 10. In the models shown in Fig. 10A, two evolution lines are calculated by varying the values of r (ratio rate of assimilation over rate of crystallization) and D^{Sr} in the De Paolo (1981) equations until a best fit is achieved encompassing the observed variability. The best fit between the models and natural data is achieved for a constant value of $r = 0.5$, because with lower r values the required variability of isotopic ratios could not be obtained. Accordingly, the two evolution lines represent the two extremes for a set of models with intermediate values for D^{Sr}. In Fig. 10B and C the evolution lines for Rb and Ba were calculated by varying the values of the bulk partition coefficients for the two elements, and keeping r and D^{Sr} values unchanged (Fig. 10A). It is shown that the MFC modeling could be considered satisfactory for explaining the evolution of the H-BG rocks. Note that the Nd isotopic systematics does not change the results, although more scatter is present.

It is noteworthy that the interaction processes had no deep effects on the bulk of the Mt. Bukulja pluton. The pluton is 95 % composed by two-mica granites which show no evidence of magma interaction. A possible reason that magma interaction processes were restricted to relatively small parts of the pluton can be related to rheological differences between magmas, *i.e.* to strong thermal and rheological contrasts between the mafic and felsic magmas. These contrasts are particularly active during the first stages of the interaction process when the mafic magma is supercooled in contact with the felsic one and thereby forced to crystallize. If the amount of mafic magma is not high the rheological behaviour is near solid, and fragmentation and dispersion of the mafic magma into the felsic one is very poor (Sparks & Marshall, 1986; Poli *et al.*, 1996). In such a way, the evidence of interaction processes remains restricted to the basic end-member, as in the Mt. Bukulja pluton (*e.g.* Christofides *et al.*, 2007).

Origin and evolution of TMG

A pure fractionation or variations in degrees of partial melting of a common source cannot be responsible for the observed geochemical trends of TMG. This is ruled out because of variable Sr and Nd isotope ratios, which, in turn, cannot be explained by variable ^{87}Rb and ^{147}Sm concentrations. It is more probable that the compositional patterns were produced by open system processes like magma interaction or crustal contamination. As mentioned above, the role of magma interaction is disfavored because the TMG rocks lack field and petrographic evidence of physical interaction of magmas of different compositions. This can be also inferred from crosscutting trends displayed by H-BG and TMG samples on some major and trace element variation diagrams (Fig. 5 and 6). Indeed, magma mixing processes have played a role during the Tertiary magmatism of the Balkan Peninsula (Prelević *et al.*, 2004), but these processes commonly result in hybrid magmas of metaluminous rather than peraluminous compositions as observed in TMG.

Alternatively, the evolution of TMG rocks involving crustal contamination processes seems more likely. We tested whether the observed geochemical variations among the TMG samples might have resulted from AFC processes, by using the approach of De Paolo (1981). The average composition of the two least evolved TMG samples (BK111 and BK115) has been taken as the parental magma composition, while sample BK136 of the metamorphic basement has been adopted as a possible contaminant. The results of the modeling are presented in Figs. 11 and 12. In the models in Fig. 11, two evolution lines are calculated by varying the values of r, D^{Sr} and D^{Nd} in the De Paolo (1981) equations until a best fit is achieved encompassing the observed variability. The best fit between

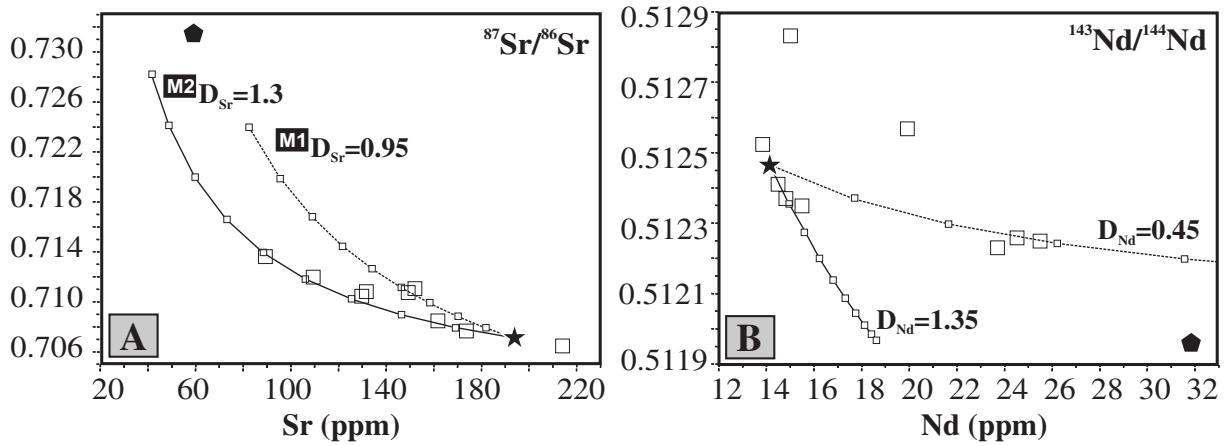

Fig. 11. $^{87}Sr/^{86}Sr_i$ *vs.* Sr (ppm) (A) and $^{143}Nd/^{144}Nd_i$ *vs.* Nd (ppm) (B) showing the two AFC models needed to encompass the variability of composition of the TMG rocks. Modelled bulk partition coefficients D for Sr and Nd are also given. Solid star – parental end-member (average composition of most primitive TMG rocks); solid pentagon – acid end-member (BK136 belonging to MB); tick marks are reported at 10 % intervals of crystal fractionation. Other symbols as in Fig. 2.

the modeled and natural data is achieved for a constant value of $r = 0.5$, because lower r values could not reproduce the required variability of isotopic ratios. The two evolution lines bound a set of models with intermediate values for D^{Sr} and D^{Nd}. They are labeled M1 and M2 to denote the models with lower and higher bulk partition coefficients, respectively. In Fig. 12 M1 and M2 evolution lines were calculated by varying the values of bulk partition coefficients for different elements, and keeping *r* and D^{Sr} constant to the values reported in Fig. 11. The results show that the AFC modeling could be considered robust for explaining evolution of the TMG rocks. In order to better constrain the model, the percentage of minerals in the fractionating assemblage has been calculated starting from the modeled bulk partition coefficients and using partition coefficients from the literature (GERM data set, http://earthref.org/GERM/main.htm; De Albuquerque, 1975, Icenhower & London, 1995, Konings *et al*., 1988 for muscovite). A linear programming minimizing the sum of squares of residuals (SSR; *e.g.* Wright & Doherty, 1970) has been used. Calculated fractionating assemblages are similar for the two models M1 and M2, and are dominated, in average, by quartz (~60 %), plagioclase (~15 %), K-feldspar (~7 %) and biotite (~7 %). Muscovite is not reported as a fractionating mineral because the amount of such a phase calculated by the least-squares modeling is very low for both M1 and M2 models. Because available partition coefficients for muscovite are sparse, this result could be taken as a first approximation, even if we must take into account that muscovite can fractionate in viscous magmas with great difficulty. In addition, the presence of different amounts of accessory minerals as titanite, apatite and zircon is necessary for elements such as Nd, La, Zr, and Y (apatite 1 and 1.5 %, titanite 0.6 and 0, zircon 0.1 and 0.07 for models M1 and M2, respectively). The involvement of such a major and accessory mineral assemblage in the AFC modeling agrees with the observed petrographic features of the TMG rocks. A fractionating mineral association containing substantial amounts of feldspars is also inferred by an increase of negative europium anomaly with decreasing of Sr concentrations (Tables 4 and 5).

However, for some elements, such as Y, Zr, REE, and Nb (not shown) data points display some scattering (Fig. 11 and 12), whereas in some cases the AFC model is unable to fit the sample variability. As stated above, Nb, Y, Zr and REE are mainly hosted in accessory minerals which are typically very inhomogeneously distributed in evolved rocks, such as TMG. Even small variations in absolute abundances of these minerals can cause a large variability of concentrations of the above mentioned elements. Therefore, we suggest that the scattering in the graphs and the inability of the AFC model to reproduce the variations of some elements is mainly due to the inhomogeneous distribution of accessory minerals in the TMG samples.

The AG rocks show very evolved character having $SiO_2 > 73$ % and most major elements < 1 %, a very high Rb/Sr ratio, and high Nb abundances indicating that they are the result of extreme degrees of fractionation starting from TMG magmas (*e.g.* Poli, 1992).

Quite high ratios of assimilated to crystallized mass (ρ = 20–50 %; Aitcheson & Forrest, 1994) suggest that substantial crustal amounts are required for the evolution of TMG. This implies that the assimilation probably involved bulk partial melting of the surrounding rocks. Similar crustal proportions were suggested by Harangi *et al*. (2001) for the petrogenesis of Middle Miocene garnet-bearing acidic rocks of the northern Pannonian Basin, that have Sr-Nd isotopic pattern similar to those of the TMG rocks (Fig. 8).

Taking into account the above presented evolutionary model we now attempt to address the origin of the least evolved TMG samples (BK111 and BK115), which were used as end-members in the AFC model. These samples could derive either by evolution processes from less evolved magmas or by crustal anatexis.

TMG primitive magmas could derive by evolution processes similar to those leading to the H-BG rocks. This hypothesis seems unlikely because, as discussed above, the H-BG rocks of the Mt. Bukulja pluton have compositions

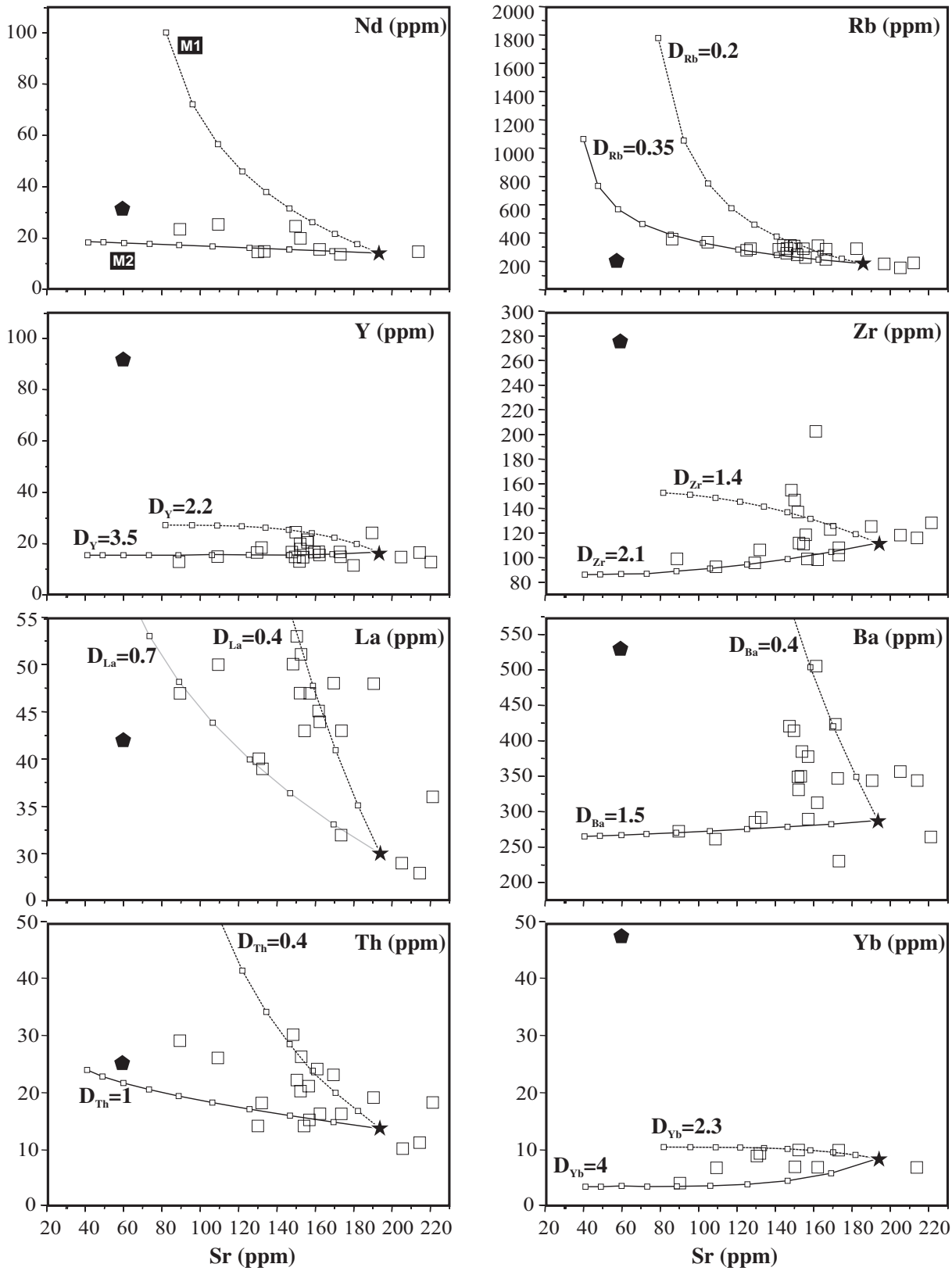

Fig. 12. Binary diagrams showing the two AFC models M1 and M2 needed to encompass the variability of composition of the TMG rocks. Modelled bulk partition coefficients D for elements are also given. D values for Sr and Nd as in Fig. 11. Solid star – parental end-member (average composition of the most primitive TMG rocks); solid pentagon – acid end-member (BK136 belonging to MB); tick marks are reported at 10% intervals of crystal fractionation. Other symbols as in Fig. 2.

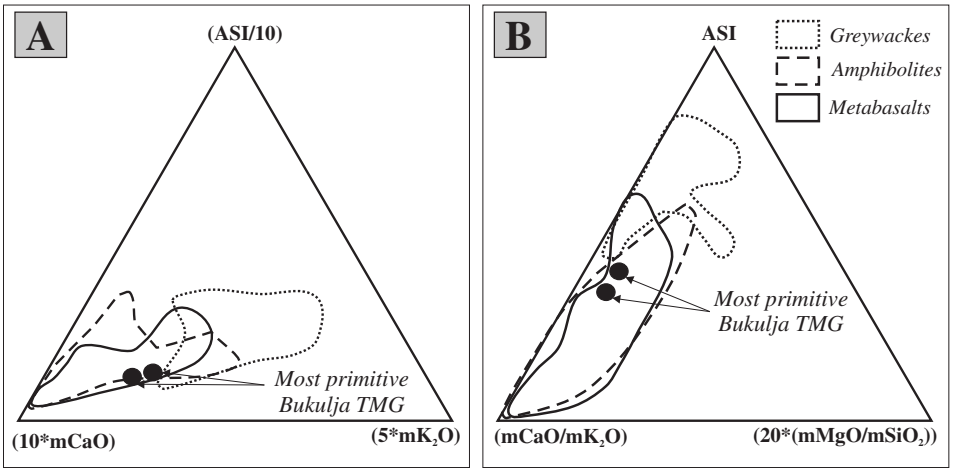

Fig. 13. ASI/10–10*CaO–5*K_2O molar (A) and ASI–CaO/K_2O–20*(MgO/SiO_2) (molar) (B) triangular diagrams displaying the composition of the most primitive TMG compared with experimental data of melt compositions from different crustal protoliths. Data are as follows for the various sources: greywackes and pelites (Montel & Vielzeuf, 1997; Patino Douce & Beard, 1996; Gardien *et al*., 1995; MacRae & Nesbitt, 1980; Carrington & Watt, 1995; Pickering & Johnston, 1998); gneisses (Patino Douce, 1997; Beard *et al*., 1994; Gardien *et al*., 1995); amphibolites (Beard & Lofgren, 1991; Rushmer, 1991; Johannes & Holtz, 1996; Wolf & Wyllie, 1994); basalts (Rapp, 1995; Rapp & Watson, 1995). In average, the degree of melting varies from minimum melts to *ca.* 20 %.

that mainly plot off the evolution line shown by the TMG samples (Fig. 9). A further hypothesis is that TMG primitive magmas could derive by simple fractional crystallization processes starting from parental magma similar to BLD, which is the only basic material present in the area. However, the composition of residual liquids after fractional crystallization calculated using MELTS software does not approach the compositions of the TMG rocks under any condition of oxygen buffer and pressures. In addition, modeling using trace elements shows that the process would require very high degrees of fractionation, higher than 80 %, which is consistent with the very low contents of compatible elements, but inconsistent with the not extremely depleted nature of the least evolved TMG samples (*e.g.* CaO > 3 %).

Fractional Crystallization coupled with crustal assimilation (AFC) processes starting from BLD could account for the ASI composition of TMG primitive magmas, assuming a crustal contaminant high in ASI. However modellization shows that to derive SiO_2 contents ~70 wt.% and very low compatible elements (Table 4) would require huge proportions of crustal material and this, in turn, would not match the observed relatively low Sr isotope ratios (~0.7065 and ~0.7077). On the other hand TMG primitive magmas cannot derive by AFC processes starting from H-BG group rocks because of different evolution lines shown by H-BG and TMG group (Fig. 9).

Although the above lines of reasoning suffer from difficulties inherent to the restricted geochemical compositions of so evolved samples, which do not permit the use of more detailed models, we assume that the composition of the least evolved TMG samples (BK111 and BK115) can be regarded as close in composition to primitive melts derived by crustal melting. To examine such a hypothesis these samples are plotted in the ternary graphs shown in Fig. 13 along with data of melt compositions obtained by melting experiments of crustal protoliths. The graph shows that the composition of the TMG samples overlaps with those of melts derived from metabasalts and amphibolites and departs from those of melts produced by melting of greywackes and pelites. This implies that rocks of intermediate-basaltic compositions (amphibolites and basalts), probably situated in middle-lower crustal levels, may serve as suitable candidates for a possible source for the least evolved TMG magma. Two observations corroborate this hypothesis: i) despite the occurrence of muscovite, the values of alumina-saturation index for these rocks (*ca.* 1) are below those of typical peraluminous magmas derived by partial melting of upper crustal sources (Sylvester, 1998), and ii) the relatively low isotopic values indicate melting of a young crust and this could be suitably represented by a lower crustal intermediate-basaltic lithology like basalts and amphibolites, rather than a metasedimentary source. This can indicate that the TMG primary magmas probably originated by melting of previous basaltic underplatings within the local lower crust. In Fig. 9 strontium isotopic compositions of the least evolved TMG samples plot close to the lower end of the Sr-isotopic range for Serbian Tertiary basalts (Cvetković *et al.*, 2004b). The behavior of the Nd isotopic composition is similar. Accordingly, melting of a basaltic rock similar in composition to the Serbian Tertiary basalts can produce acid/intermediate metaluminous to slightly peraluminous melts which would have a Sr and Nd isotope signature similar to that observed in the least evolved TMG rocks.

Summary and conclusions

The Miocene pluton of Mt. Bukulja is predominantly composed of two-mica granite with small amount of more mafic lithologies. The emplacement of the granitic magma occurred between 20 Ma and 17 Ma. The available petrological and geochemical data suggest that the

most primitive two-mica granite originated by partial melting of mantle-derived mafic rocks in an intermediate-lower crust, compositionally similar to the Serbian Tertiary basalts. Such anatectic melts evolved through AFC processes which have been modeled through trace element contents and Sr-Nd isotope ratios. The model suggests a high crustal contribution (20 to 50 %). Owing to the restricted sample collection of the H-BG group only some hypotheses have been outlined for the origin and evolution of these rocks. They might have been produced by magma interaction processes in which the basic end member was similar in composition to the lamprophyric dyke found near the Mt. Bukulja pluton, whereas the felsic end-member was a restricted batch of the TMG magma.

The petrologic characteristics and the geographic position of the Mt. Bukulja pluton suggest that it can be geotectonically related to the Pannonian extension, in contrast to other granitoids of the Dinarides that are predominantly Oligocene in age and metaluminous in composition. If granitoid magmatism of Mt. Bukulja originated in response to the tectonic evolution of the Pannonian Basin, then it should be a possible counterpart of the 21–16 Ma acid calc-alkaline volcanism of the northern Pannonian Basin. This volcanism produced widespread ignimbritic sheets of rhyolitic composition as well as garnet-bearing rhyodacites and andesites, presently occurring in north Hungary (Poka *et al*., 1998; Harangi, 2001; Harangi *et al*., 2001). Evidence suggesting a link between the Mt. Bukulja granite and acid volcanics in north Hungary are several: (1) TMG and north Hungary volcanic rocks have the same age which coincides with the period of counterclockwise rotation of the Alcapa block (Márton, 1987) and with the initiation of a 200 km back-arc extension at the southern border of the Central Western Carpathians (Frisch *et al*., 2000); (2) the compared rocks show a very similar Sr-Nd isotope signature and trace element patterns (Fig. 7 and 8); (3) the crustal component has been found to play a significant role in the evolution of both Mt. Bukulja granite and north Hungary volcanics; (4) the Mt. Bukulja granitoid intrudes Paleozoic rocks of the Jadar block terrane, whereas the north Hungary volcanics overlay metamorphic rocks of the Mt. Bükk unit, and both units are interpreted as tectonic blocks with the same pre-Tertiary tectonostratigraphic history (Protić *et al*., 2000). Point three is particularly striking because accentuated contribution of crustal sources requires a very high heat flow which can be related to updoming of hot mantle material beneath the Pannonian Basin. This is also inferred from recent heat flow estimates of around 100 mW/m^2 and determinations of lithospheric thickness of around 60 km (Adam & Wesztergom, 2001).

Therefore, we conclude that the Mt. Bukulja TMG and Early/Middle Miocene acid volcanic rocks of the northern part of the Pannonian Basin may have been related to a common tectonomagmatic phase and most probably they originated during the initial phase of the Pannonian extension.

Acknowledgements: This paper is dedicated to the late Prof. Vera Knežević-Đordević for her decades of work on Serbian granites and to whom we all are endlessly grateful for friendship and support. We thank F. Parat and R. Trumbull for their constructive comments that significantly improved the paper. Editorial handling by D. Lattard and A. Peccerillo was very helpful. This study has been supported by the Italian Ministry of Science and the University of Perugia. V.C. and K.Š. thank the Ministry of Science and Environment Protection of the Republic of Serbia, Project No. 146013 and to the Serbian Academy of Sciences and Arts (Geodynamic Project) for financial support.

Appendix – Analytical techniques

Modal analyses were performed using a classical point counting method, using a Swift-pointcounter making between 1500 and 2500 points for each thin section.

Mineral analyses were performed by Energy Dispersive Spectrometry at the University of Thessaloniki (Greece) using a LINK-EDS microanalyser attached to a Jeol JSM-840 Scanning Electron Microscope. The operating conditions were: 15 kV accelerating potential, 3 nA beam current, beam 1 μm^2, 80 s counting time. A ZAF-4/FLS software was used for corrections and natural minerals and pure metals were used as standards. Standardized quantification accuracy is mostly better than ±0.5 %.

Age analyses were performed in the K/Ar Laboratory of the Institute of Nuclear Research of Hungarian Academy of Sciences (ATOMKI) (Debrecen, Hungary). Samples were crushed and then a split of the crushed rocks was selected and pulverized for potassium determination. Approximately 500 mg of each sample was used for Ar analyses. The samples were degassed by high-frequency induction heating, and the conventional getter materials were used for cleaning Ar. The ^{38}Ar spike was introduced to the system from a gas pipette before degassing. The cleaned Ar was directly introduced into the mass spectrometer, operated in the static mode. Recording and evolution of Ar spectra was controlled by a microcomputer. Approximately 100 mg of the pulverized material was digested in HF with the addition of some sulphuric and perchloric acids. The digested samples were dissolved in 100 ml 0.25 mol/1 HCl and diluted fivefold. Na and Li (100 ppm) were added as buffer and internal standard. K concentration was measured with a digitalized flame photometer. The interlaboratory standards HD-B1, GL-O, LP-6 and Asia 1/65 were used for calibration. Details of the instruments, applied methods and results of calibration have been described by Balogh (1985).

Major and trace element analyses were performed on crushed samples starting from *ca.* 5 kg of material. Major elements (exclusive of FeO, MgO and LOI determined by wet chemical analyses) were analyzed by X-ray fluorescence spectrometry (XRF) with full matrix correction after Franzini & Leoni (1972); Cr, V, Ni, Co, Ga, Rb, Sr, Y, Zr, Nb, Ba, La, Ce, Pb, and Th by XRF after Kaye (1965). Precision is better than 15 % for V, Ni, better than 10 % for Co, Cr, Y, Zr, Ba, and better than 5 % for all other elements. U, Sc, Cs, Hf, Ta, Cr, Co and REE have been determined at the Department of Earth Sciences, University of Western

Ontario, by instrumental neutron activation analysis after Gibson & Jagam (1980). Precision is better than 10 % for most elements, except for Nd and Cs which is about 15 %. The accuracy has been tested on international standards and is better than 10 %.

Isotope analyses were performed at the Atlantic Universities Radiogenic Isotope Facility (Canada) with a Finnigan MAT 262V TI. Replicate analyses of NBS RSM 987 and La Jolla standards allowed to estimate an external reproducibility better than 2×10^{-5}. Uncertainties in measured and initial isotopic ratios represent ± 2□ run precision and ±2□ error propagation, respectively.

References

Adam, A. & Wesztergom, V. (2001): An attempt to map the depth of the electrical asthenosphere by deep magnetotelluric measurements in the Pannonian basin (Hungary). *Acta Geol. Hung*., **4**, 167-192.

Aitcheson, S.J. & Forrest, A. H. (1994): Quantification of crustal contamination in open magmatic systems. *J. Petrol*., **35**, 461-488.

Asimow, P. D. & Ghiorso, M. S. (1998): Algorithmic modifications extending MELTS to calculate subsolidus phase relations. *Am. Mineral*., **83**, 1127-1132.

Balogh, K. (1985): K/Ar dating of Neogene volcanic activity in Hungary: experimental technique, experiences and methods of chronological studies. *ATOMKI, Annual Report* **D/1**, 277-288.

Beard, J.S. & Lofgren, G.E. (1991): Dehydration melting and watersaturated melting of basaltic and andesitic greenstones and amphibolites at 1, 3 and 6.9 Kb. *J. Petrol*., **32**, 365-401.

Beard, J.S., Lofgren, G.E., Sinha, A.K., Tollo, R.P. (1994): Partial melting of apatite bearing charnockite, granulite, and diorite: melt composition, restite mineralogy and petrologic implications. *J. Geophys. Res*., **99**, 21591-21603.

Carrington, D.P. & Watt, G.R. (1995): A geochemical and experimental study of the role of K-feldspar during water-undersaturated melting of metapelites. *Chem. Geol*., **122**, 59-76.

Christofides, G., Perugini, D., Koroneos, A., Soldatos, T., Poli, G., Eleftheriadis, G., Del Moro, A., Neiva, A.M. (2007): Interplay between geochemistry and magma dynamics during magma interaction: An example from the Sithonia Plutonic Complex (NE Greece). *Lithos* **95**, 243-266.

Cvetković, V., Knežević, V., Christofides, G., Koroneos, A., Poli, G. (2004a): Origin, evolution and geotectonic setting of granitoid rocks of Cer Mt. (western Serbia). Extendend Abstract of the 10th International Congress of the Geological Society of Greece, Thessaloniki, Greece, 15 to 17 April 2004, 372-373.

Cvetković, V., Prelević, D., Downes, H., Jovanović, M., Vaselli, O., Pécskay, Z. (2004b): Origin and geodynamic significance of Tertiary postcollisional basaltic magmatism in Serbia (Central Balkan Peninsula). *Lithos*, **73**, 161-186.

De Albuquerque, C.A.R. (1975): Partition of trace elements in coexisting biotite, muscovite and potassium feldspar of granitic rocks, Northen Portugal. *Chem. Geol*., **16**, 89-108.

Deer, W.A., Howie, R.A. & Zussman, J. (1978): Rock Forming Minerals, 2nd ed. *Wiley, New York.*, 696 p.

Deleon, G. (1969): Pregled rezultata određivanja apsolutne geološke starosti granitoidnih stena u Jugoslaviji. *Radovi Instituta za Geološka i Rudarska Istraživanja Beograd*, 6, 165-182.

De Paolo, D.J. (1981): Trace element and isotopic effects of combined wall rock assimilation and fractional crystallisation. *Earth Planet. Sci. Lett*., **53**, 189-202.

Didier, J., & Barbarin B. (1991): The different types of enclaves in granites: nomenclature. *in* "Enclaves and granite petrology", Didier, J., & Barbarin B., (ed.) Elsevier International, Amsterdam-New York, Developments in Petrology 13, 19-23.

Divljan, S., & Cvetić, S. (1991): Prilog poznavanju osnovnih petrološko-geoloških karakteristika tercijarnih magmata šireg područja Šumadije. *Bulletin of Natural History Museum in Belgrade*, **A46**, 95-114.

Erić, V. (1999): Petrology and geochronology of granitoids and uran mineralization of Bukulja. *MSc thesis, Faculty of Mining and Geology, University of Belgrade*, 112 p.

Franzini, M. & Leoni, L. (1972): A full matrix correction in X-ray fluorescence analysis of rock samples. *Atti Soc. Toscana Sci. Nat., Ser A*., **79**, 7-22.

Frisch, W., Dunkl, I., Kuhlemann, J. (2000): Post-collisional orogen-parallel large-scale extension in the Eastern Alps. *Tectonophysics*, **327**, 239-265.

Gardien, V., Thompson, A.B., Grujic, D., Ulmer, P. (1995): Experimental melting of biotite+plagioclase+quartz+or — muscovite assemblages and implications for crustal melting. *J. Geophys. Res*., **B 100**, 15581-15591.

Ghiorso, M. S. & Sack, R.O. (1995): Chemical mass transfer in magmatic processes; IV, A revised and internally consistent thermodynamic model for the interpolation and extrapolation of liquid-solid equilibria in magmatic systems at elevated temperatures and pressures. *Contrib. Mineral. Petrol*., **119**, 197-212.

Gibson, I.L. & Jagam, P. (1980): Instrumental neutron activation analysis of rocks and minerals. *in*: "Neutron Activation Analysis in the Geosciences", Muecke, G.K, Short Course, Mineral Ass. Canada, 109-131.

Harangi, S. (2001): Neogene to Quaternary volcanism of the Carpathian-Pannonian region; a review. *Acta Geol. Hung*., **44**, 223-258.

Harangi, S., Downes, H., Kosa, L., Szabo, C., Thirlwall, M. F., Mason, P.R.D., Mattey, D. (2001): Almandine garnet in calc-alkaline volcanic rocks of the northern Pannonian Basin (Eastern-Central Europe); geochemistry, petrogenesis and geodynamic implications. *J. Petrol*., **42**, 1813-1843.

Haskin, L.A., Frey, F.A., Schmitt, R.A., Smith, R.H. (1966): Meteoritic, solar and terrestrial rare-earth distributions. Physics and Chemistry of the Earth, *Pergamon Press, New York*, p. 167-321.

Hibbard, M.J. (1995): Petrography to petrogenesis. *Prentice Hall, Englewood Cliffs, New Jersey*, 587 p.

Icenhower, J.P. & London, D. (1995): An experimental study of element partitioning between biotite, muscovite and coexisting peraluminous granitic melt at 200 MPa (H_2O). *Am. Mineral*., **80**, 1229-1251.

Johannes, W. & Holtz F. (1996): Petrogenesis and experimental petrology of granitic rocks. *Berlin, Springer Verlag*, 335 p.

Karamata, S., Steiger, R., Đorđević, P., Knežević, V. (1990) New data on the orgin of granitic rocks from Western Serbia. *Bulletin CVIII de l'Acad. Serbe des Sciences et des Arts, Classe des Sciences naturelles et mathematiques*, **32**, 1-9.

Karamata, S., Krstić, B., Dimitrijević, M. D., Knežević, V., Dimitrijević, M. N., Filipović, I. (1994): Terranes between the Adriatic and the Carpatho-Balkan arc. *Bulletin CVIII de l'Acad. Serbe des Sciences et des Arts, Classe des Sciences naturelles et mathematiques*, **35**, 47-68.

Kaye, M.J. (1965): X-ray fluorescence determinations of several trace elements in some standard geochemical samples. *Geochim.Cosmochim. Acta*, **29**, 139-142.

Knežević, V., Steiger, R., Đorđević, P., Karamata, S. (1989): Precambrian contribution to Tertiary granitic melts at the southern margin of the Pannonian Basin. Symposium on Precambrian granitoids, August 14-17 1989, Helsinki, Finland, Abstract with program.

Konings, R.J.M, Boland, J.N., Vriend S.P., Ben, J., Jansen, H. (1988): Chemistry of biotites and muscovites in the Abas granite, northern Portugal. *Am. Mineral*., **73**, 754-765.

Leake, B. E., Woolley, A. R., Arps, C. E. S., Birch, W. D., Gilbert, M. C., Grice, J. D., Hawthorne, F. C., Kato, A., Kisch, H. J., Krivovichev, V. G., Linthout, K., Laird, J., Mandarino, J., Maresch, W. V., Nickel, E. H., Rock, N. M. S., Schumacher, J. C., Smith, D. C., Stephenson, N. C. N., Ungaretti, L., Whittaker, E. J. W., Youzhi, G. (1997): Nomenclature of amphiboles; report of the Subcommittee on Amphiboles of the International Mineralogical Association Commission on new minerals and mineral names. *Mineral. Mag*., **61**, 295-321.

MacRae, N. D. & Nesbitt, H. W. (1980): Partial melting of common metasedimentary rocks: a mass balance approach. *Contrib. Mineral. Petrol*., **75**, 21-26.

Márton, E. (1987): Paleomagnetism and tectonics in the Mediterranean region. *J. Geodyn*., **7**, 33-57.

McDonough, W.F., Sun, S.-S., Ringwood, A.E., Jagoutz, E., Hofmann, A.W. (1992). Potassium, Rubidium and Cesium in the Earth and Moon and the evolution of the mantle of the Earth. *Geochim. Cosmochim. Acta*, **56**, 1001-1012.

Miller, C.F., Stoddard, E.F., Bradfish, L.J., Dollase, W.A. (1981): Composition of plutonic muscovite: genetic implications. *Can. Mineral*., **19**, 25-34.

Montel, J.M. & Vielzeuf, D. (1997): Partial melting of metagreywackes; Part II, Compositions of minerals and melts. *Contrib. Mineral. Petrol*., **128**, 176-196.

Pamić, J. (1993): Eoalpine to Neoalpine magmatic and metamorphic processes in the northwestern Vardar Zone, the easternmost Periadriatic Zone and the southwestern Pannonian Basin. The origin of sedimentary basins; inferences from quantitative modelling and basin analysis. *Tectonophysics*, **226**, 503-518.

Pamić, J. & Balen, D. (2001): Tertiary magmatism of the Dinarides and the adjoining South Pannonian Basin: an overview. *Acta Vulcanol*., **13**, 9-24.

Patiño Douce, A.E. (1997): Generation of metaluminous A-Type granites by low pressure melting of calc-alkaline granitoids. *Geology*, **25**, 743-746.

Patiño Douce, A.E. & Beard, J.S. (1996): Effects of P, f(O_2) and Mg/ Fe ratio on dehydration melting of model metagreywackes. *J. Petrol*. **37**, 999-1024.

Pe-Piper, G. (2000): Origin of S-type granites coeval with I-type granites in the Hellenic subduction system, Miocene of Naxos, Greece. *Eur. J. Mineral*., **12**, 859-875.

Perugini, D., Poli, G., Mazzuoli, R. (2003): Chaotic advection, fractals and diffusion during mixing of magmas; evidence from lava flows. *J. Volcanol. Geoth. Res*., **124**, 255-279.

Perugini D., Poli G., Christofides G., Eleftheriadis G., Koroneos, A. & Soldatos, T. (2004): Mantle Derived and Crustal Melts Dichotomy in Northern Greece: Spatiotemporal and Geodynamic Implications. *Geol. J*., **39**, 63-80.

Pickering, J. & Johnston, A. (1998): Fluid absent melting behaviour of a two mica metapelite: experimental constraints on the origin of Black Hills Granite. *J. Petrol*., **39**, 1787-1804.

Pietranik, A., Koepke, J., Puziewicz, J. (2006): Crystallization and resorption in plutonic plagioclase: Implications on the evolution of granodiorite magma (Gesiniec granodiorite, Strzelin Crystalline Massif, SW Poland). *Lithos*, **86**, 260-280.

Poka, T., Zelenka, T., Szakacs, A., Seghedi, I., Nagy, G., and Simonits, A. (1998): Petrology and geochemistry of the Miocene acidic explosive volcanism of the Bukk Foreland; Pannonian Basin, Hungary. *Acta Geol. Hung*., **41**, 437-466.

Poli, G. (1992) Geochemistry of Tuscan archipelago granitoids, Central Italy: the role of hybridization and accessory phase crystallization in their genesis. *J. Geol.*, **100**, 41-56.

Poli, G., Tommasini, S., Halliday, A. N. (1996): Trace element and isotopic exchange during acid-basic magma interaction processes. *Trans. R. Soc. Edin.-Earth*, **87**, 225-232.

Prelević, D., Foley, S. F., Cvetković, V., Romer, R. L. (2004): Origin of minette by mixing of lamproite and dacite magmas in Veliki Majdan, Serbia. *J. Petrol*., **45**, 759-792.

Prelević, D., Foley, S. F., Romer, R. L., Cvetković, V., Downes, H. (2005): Tertiary Ultarpotassic Volcanism in Serbia: Constraints on Petrogenesis and Mantle Source Characteristics. *J. Petrol*., **46**, 1443-1487.

Protić, Lj., Filipović, I., Pelikan, P., Jovanović, D., Kovacs, S., Sudar, M., Hips, K., Less, G., Cvijić, R. (2000): Correlation of the Carboniferous, Permian and Triassic sequences of the Jadar block, Sana-Una and "Bukkium" terranes. *in* "Geology and Metallogeny of the Dinarides and the Vardar Zone" Karamata, S. & Jankovic, S. ed. Academy of Sciences and Arts of the Republic of Serbia, 1, 61-69.

Rapp, R. P. (1995): The amphibole out phase boundary in partially melted metabasalt and its control over melt fraction and composition, and source permeability. *J. Geophys. Res*., **100**, 15601-15610.

Rapp, R. P. & Watson, E. B. (1995): Dehydration melting of metabasalt at 8-32 kbar: Implications for continental growth and crust-mantle recycling. *J. Petrol*., **36**, 891-931.

Rottura, A., Del Moro, A., Caggianelli, A., Bargossi, G.M., Gasparotto, G. (1997): Petrogenesis of the Monte Croce granitoids in the context of the Permian magmatism in the Southern Alps, Italy. *Eur. J. Mineral.*, **9**, 1293-1310.

Rushmer, T. (1991): Partial melting of two amphibolites: contrasting experimental results under fluid-absent conditions. *Contrib. Mineral. Petrol*., **107**, 41-59.

Schofield, D.I. & D'Lemos R.S. (2000): Granite petrogenesis in the Gander Zone, NE Newfoundland: mixing of melts from multiple sources and the role of lithospheric delamination. *Can. J. Earth Sci*., **37**, 535-547.

Seghedi, I., Downes, H., Szakacs, A., Mason, P.R.D., Thirlwall, M. F., Rosu, E., Pecskay, Z., Márton, E., Panaiotu, C. (2004): Neogene-Quaternary magmatism and geodynamics in the Carpathian-Pannonian region: a synthesis. *Lithos*, **72**, 117-146.

Smith, P.M. & P.D. Asimow (2005): Adiabat_1ph: A new public front-end to the MELTS, pMELTS, and pH-

MELTS models. *Geochem. Geophys. Geosyst*., **6**, Q02004, doi:10.1029/2004GC000816.

Sparks, R.S.J. & Marshall, L.A. (1986): Thermal and mechanical constraints on mixing between mafic and silicic magmas. *J. Volcanol. Geoth. Res*., **29**, 99-124.

Streckeisen, A. & Le Maitre, M.R.W. (1979): A chemical approximation to the modal QAPF classification of the igneous rocks. *Neues Jahrb. Miner. Abh*., **136**, 169-206.

Sylvester, P.J. (1998): Post-collisional strongly peraluminous granites. *Lithos*, **45**, 29-44.

Trajanova, M., Pecskay, Z., Itaya, T. (2005): Timing and magmatism in the Pohorje Mts., Slovenia. Third Croatian Geological Congress, 7th Workshop on Alpine Geological Studies, Opatija, abstract with program, 97-98.

von Blanckenburg, F. & Davies, J. H. (1995): Slab breakoff: a model for syncollisional magmatism and tectonics in the Alps. *Tectonics*, **14**, 120-131.

Wolf, M.B. & Wyllie P.J. (1994) Dehydration melting of amphibolite at 10 kbar: the effects of temperature and time. *Contrib. Mineral. Petrol*., **115**, 369-383.

Wright, T.L. & Doherty, P.C. (1970): A linear programming and least squares computer method for solving petrologic mixing problems. *Geol. Soc. Am. Bull*., **81**, 1995-2007.

Received 22 June 2006
Modified 26 January 2007
Accepted 7 May 2007